Anpassung an Temperatur Mechanismen der Temperaturregulierung II

Wärmeaustauscher

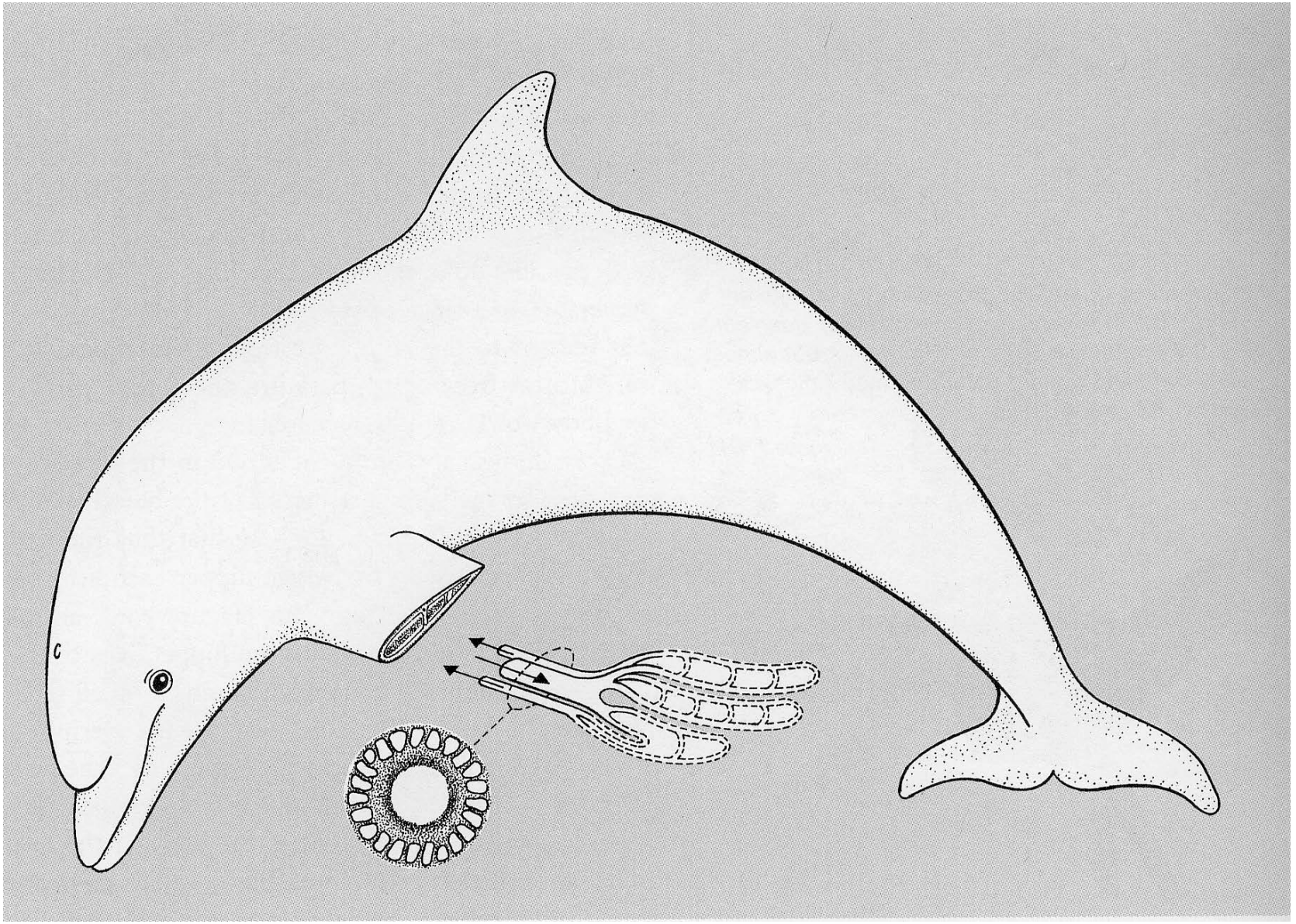

Schmidt-Nielsen 1997. Animal Physiology. 5th ed. Cambridge UUP, Cambridge UK.

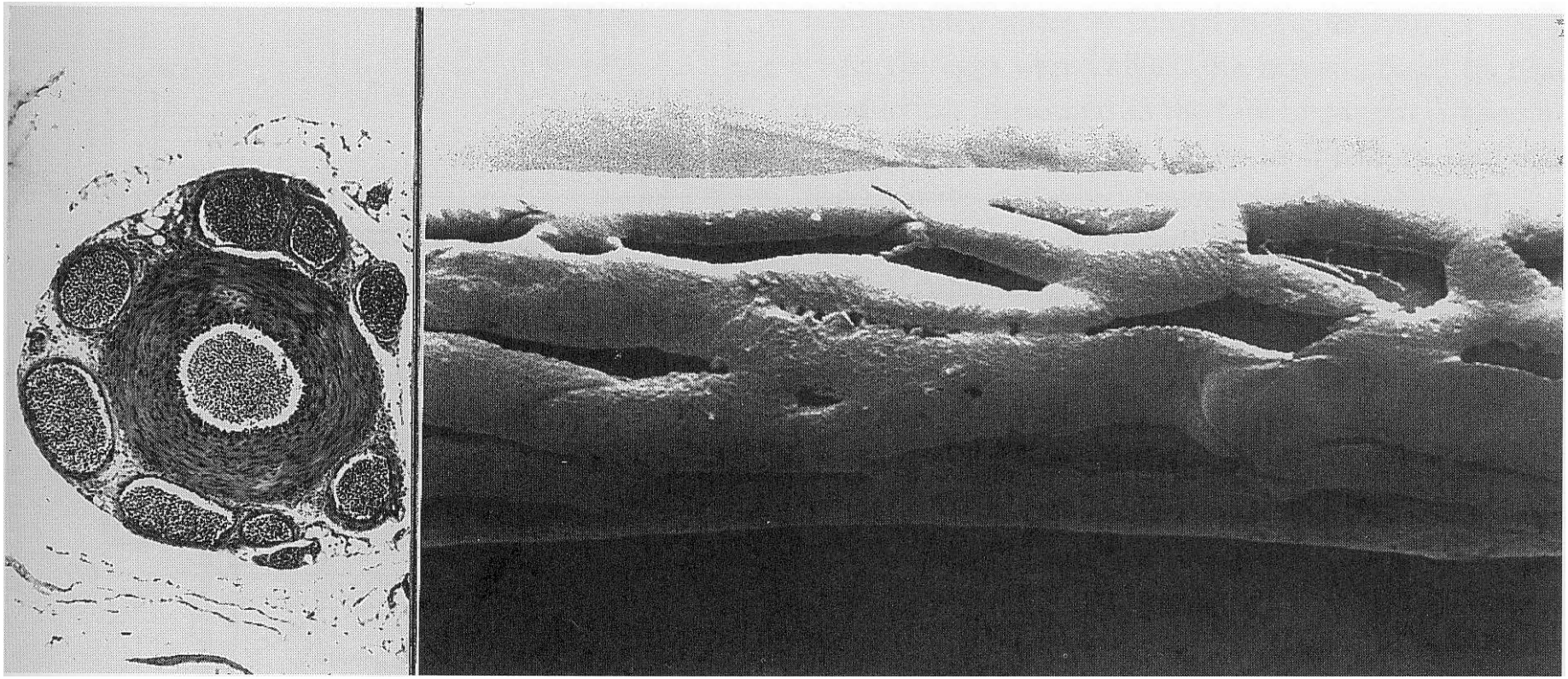

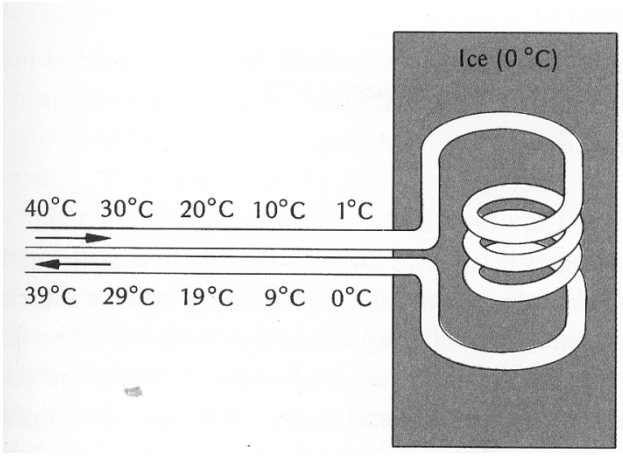

Wärmeaustausch im Gegenstromprinzip

Schmidt-Nielsen 1997. Animal Physiology. 5th ed. Cambridge UUP, Cambridge UK.

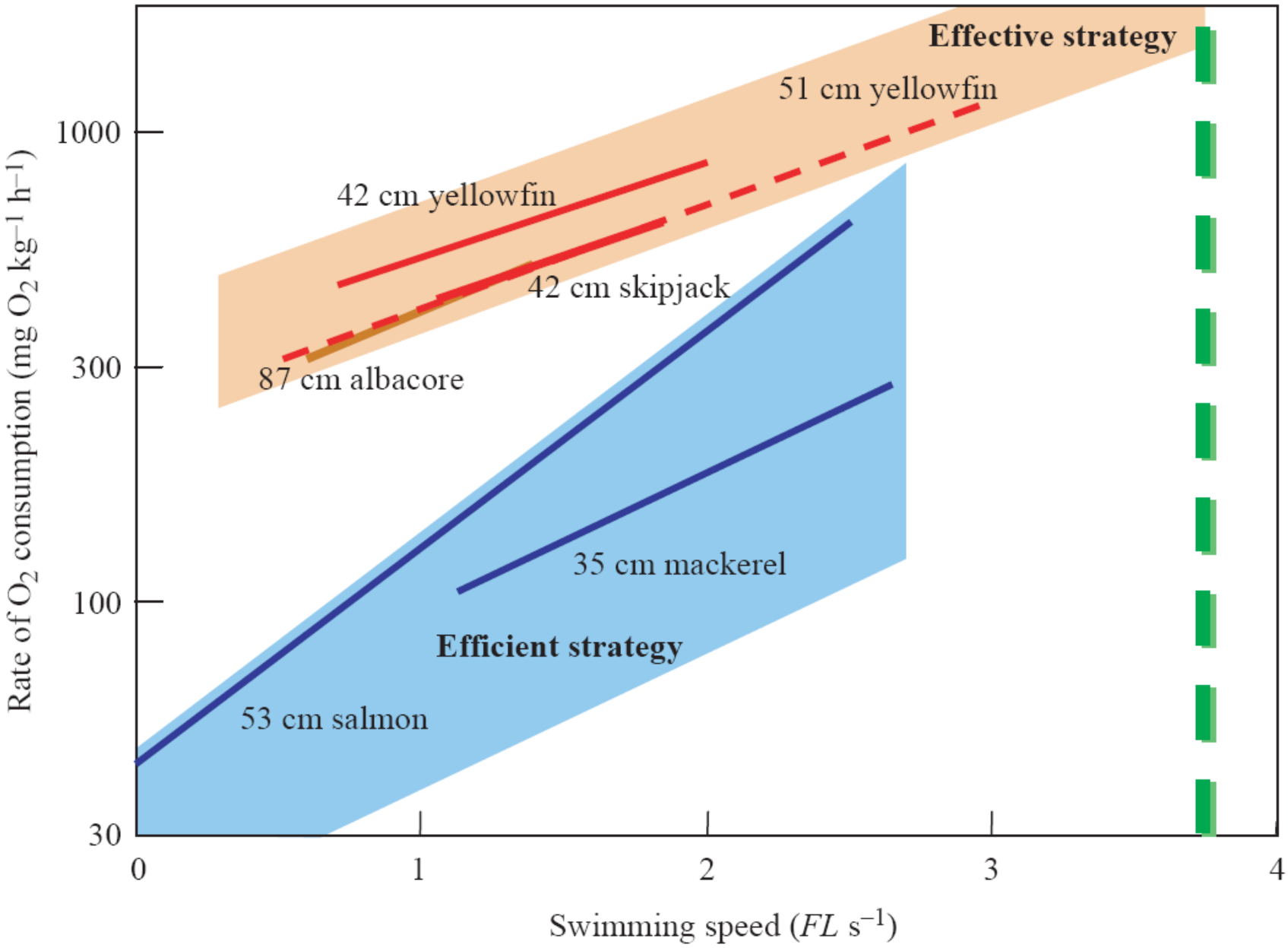

Katz 2002. Design of heterothermic muscle in fish. J. exp. Biol. 205, 2251-2266.

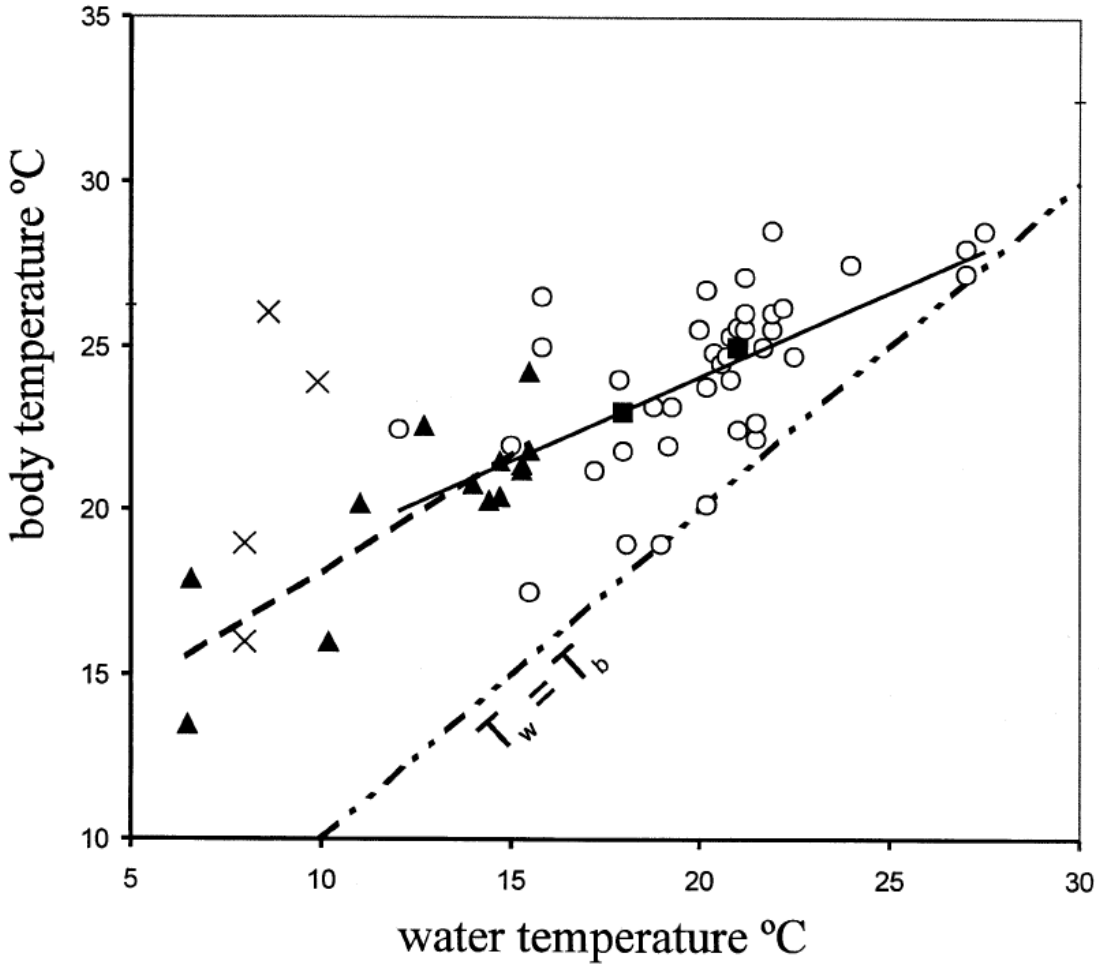

Fig. 9. Relationship between the body temperature (T_b) and surface water temperature (T_w) in lamnid sharks. Regression equations for *Isurus oxyrinchus* (○) 0.51 T_w + 13.8, $r^2 = 0.62$, $n = 38$ (solid line); *Lamna nasus* (▲) 0.72 T_w + 10.8, $r^2 = 0.68$, $n = 13$ (dashed line). Other species: *Lamna ditropis* (X), *Carcharodon carcharias* (■). Sources: Carey and Teal (1969a), Rhodes and Smith (1983), Block and Carey (1985), Carey et al. (1985), and Bernal and Graham (personal observation).

Bernal et al. 2001. CBP part A 129. 695-726.

Thunfisch Muskulatur

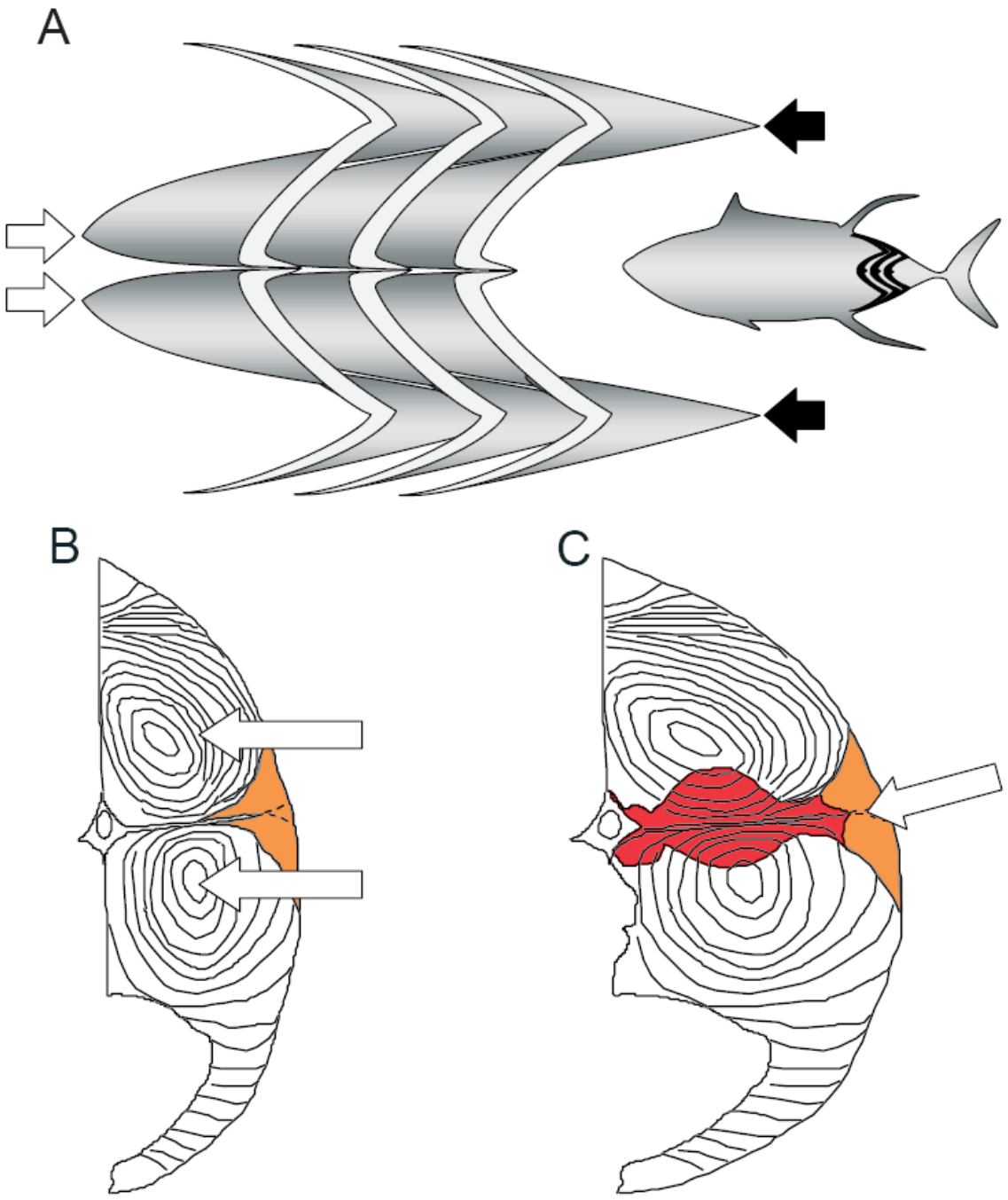

Katz 2002. Design of heterothermic mnuscle in fish. J. exp. Biol. 205, 2251-2266.

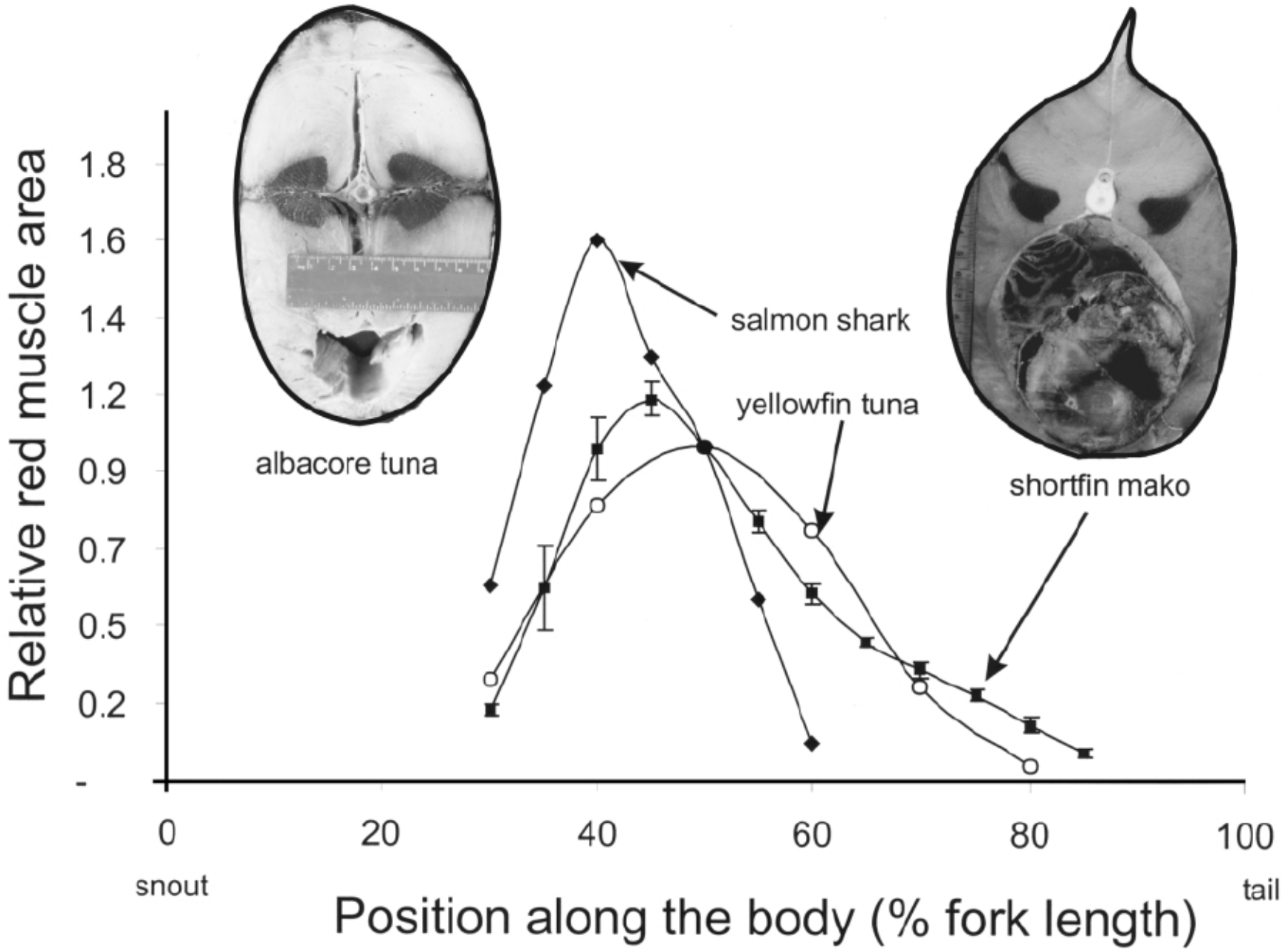
Relative red muscle area
1.8
1.6
1.4
1.2
0.9
0.7
0.5
0.2
-
albacore tuna
salmon shark
yellowfin tuna
shortfin mako
0
20
40
60
80
100
snout
tail
Position along the body (% fork length)

Muskulatur und Gefäßversorgung in yellowfin und bluefin Thunfisch

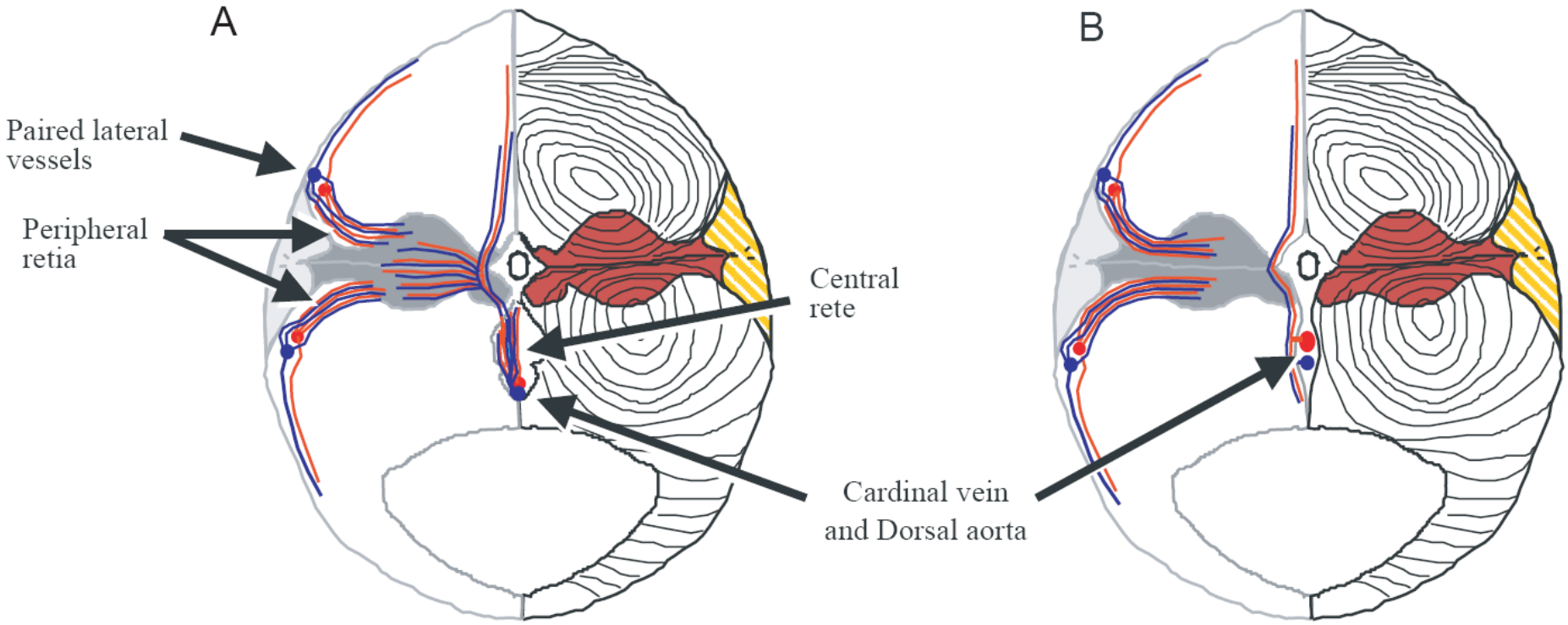

Thunnus albacares
(Yellowfin)

Thunnus thunnus
(Bluefin)

Katz 2002. Design of heterothermic muscle in fish. J. exp. Biol. 205, 2251-2266.

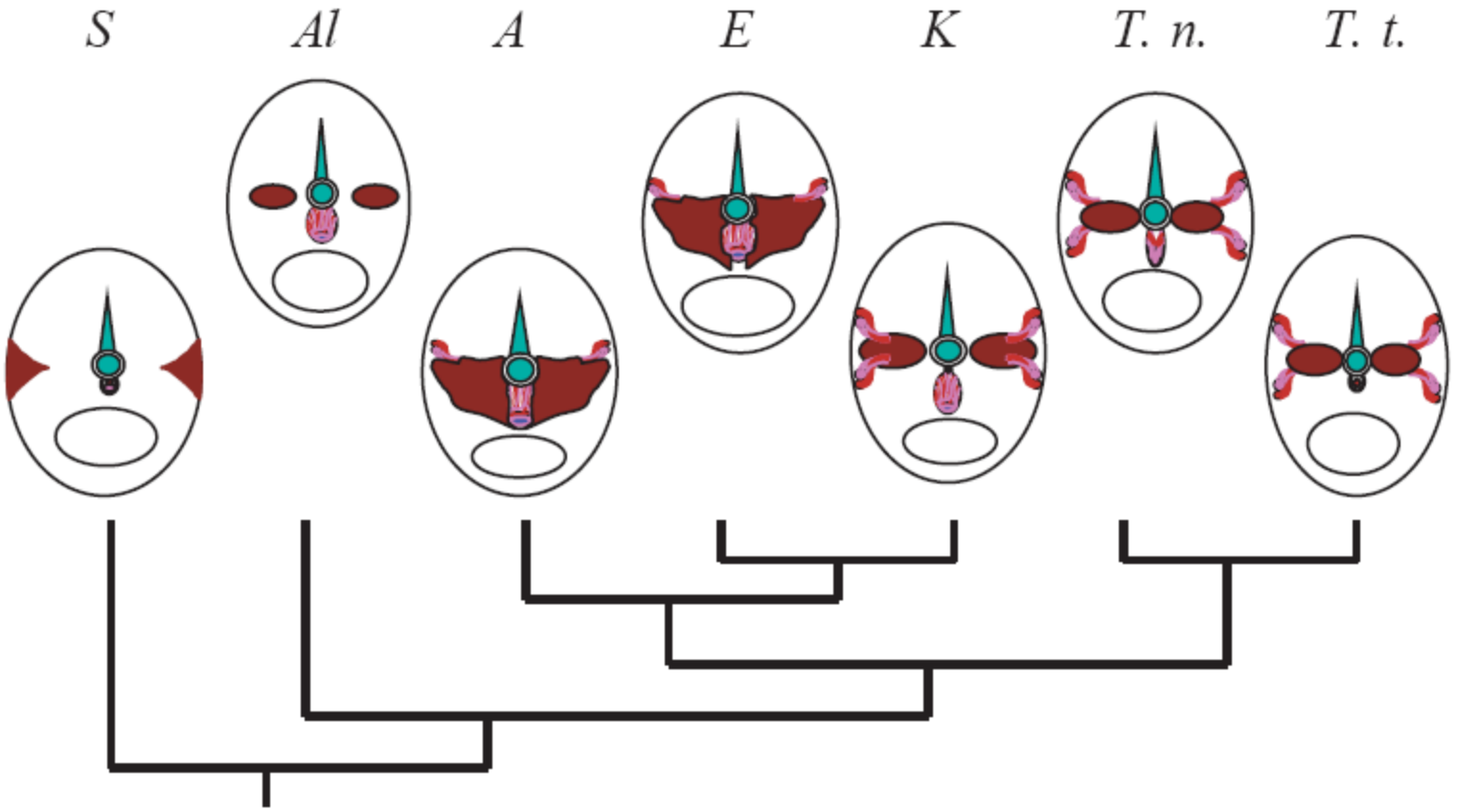

Fig. 7. Cladogram for *Sarda* and the five tuna genera (abbreviations as above) reflecting differences in the position and the relative quantity (as illustrated in near mid-body transverse sections) of RM (deep red), and the phyletic trend for greater emphasis on lateral vascular supply [arteries (red), veins (blue)] and *retia* (red and blue lines) for RM. See text for detail.

Graham and Dickson 2004. Tuna comparative physiology. J. exp. Biol. 4015-4024

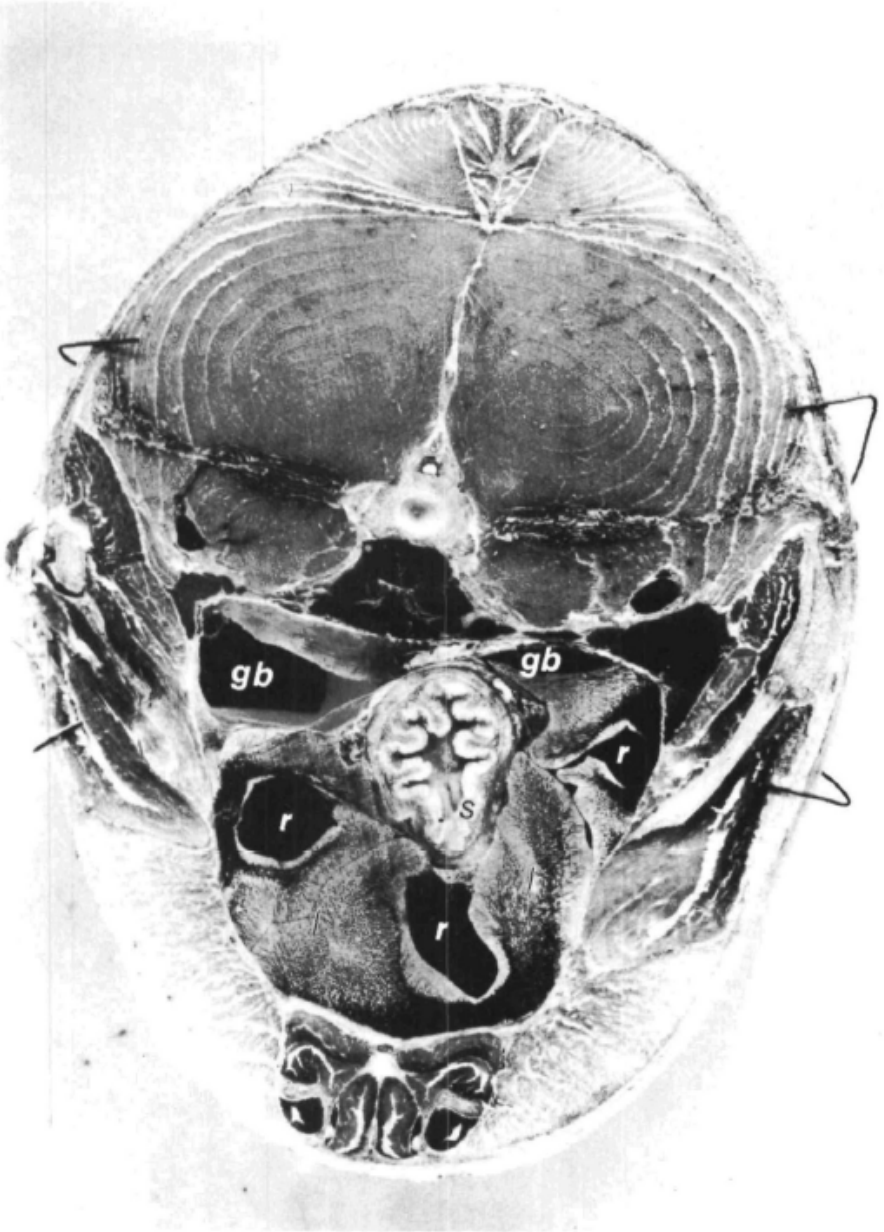

Fig. 9. Cross-section of a bluefin tuna just anterior to the origin of the pectoral fins. The viscera slumped to the right side as the tuna was frozen and the gas bladder (*gb*) which should extend evenly over the top of the body cavity, was pushed to the left side. The viscera are insulated from the warm swimming muscles by the gas bladder and from the cold water by the thick fatty muscle of the body wall. Blood is supplied to the visceral organs through a system of retia mirabilia (*r*) which are in three main groups on the back of the liver (*l*). The stomach (*s*) is thermally isolated in the centre of the fish.

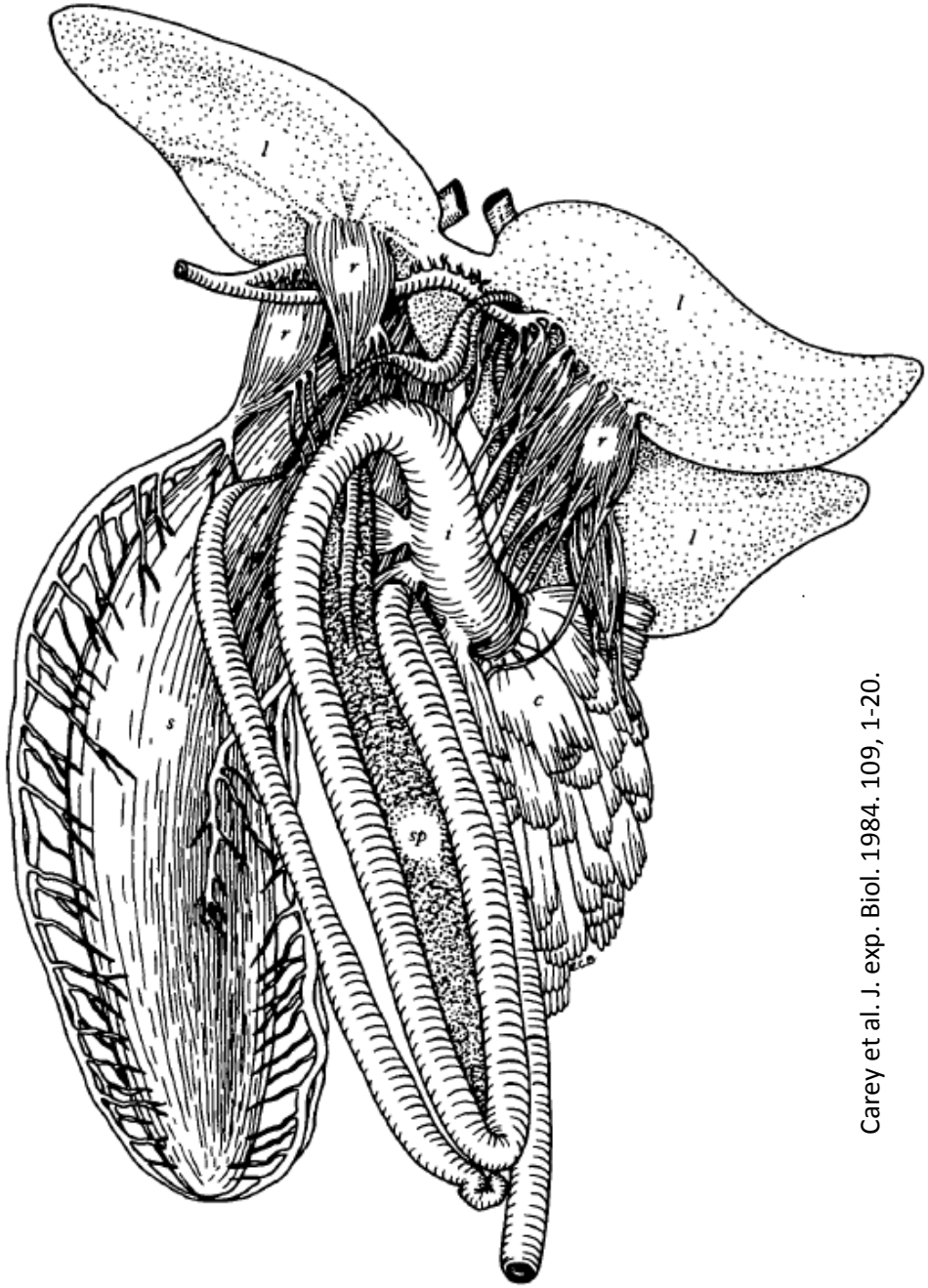

Fig. 8. Digestive organs and retia from a bluefin tuna redrawn from Eschricht & Müller, 1835. The large retia (*r*) behind the liver (*l*) supply blood to the stomach (*s*), intestine (*i*), spleen (*sp*) and pyloric caeca (*c*).

Carey et al. J. exp. Biol. 1984. 109, 1-20.

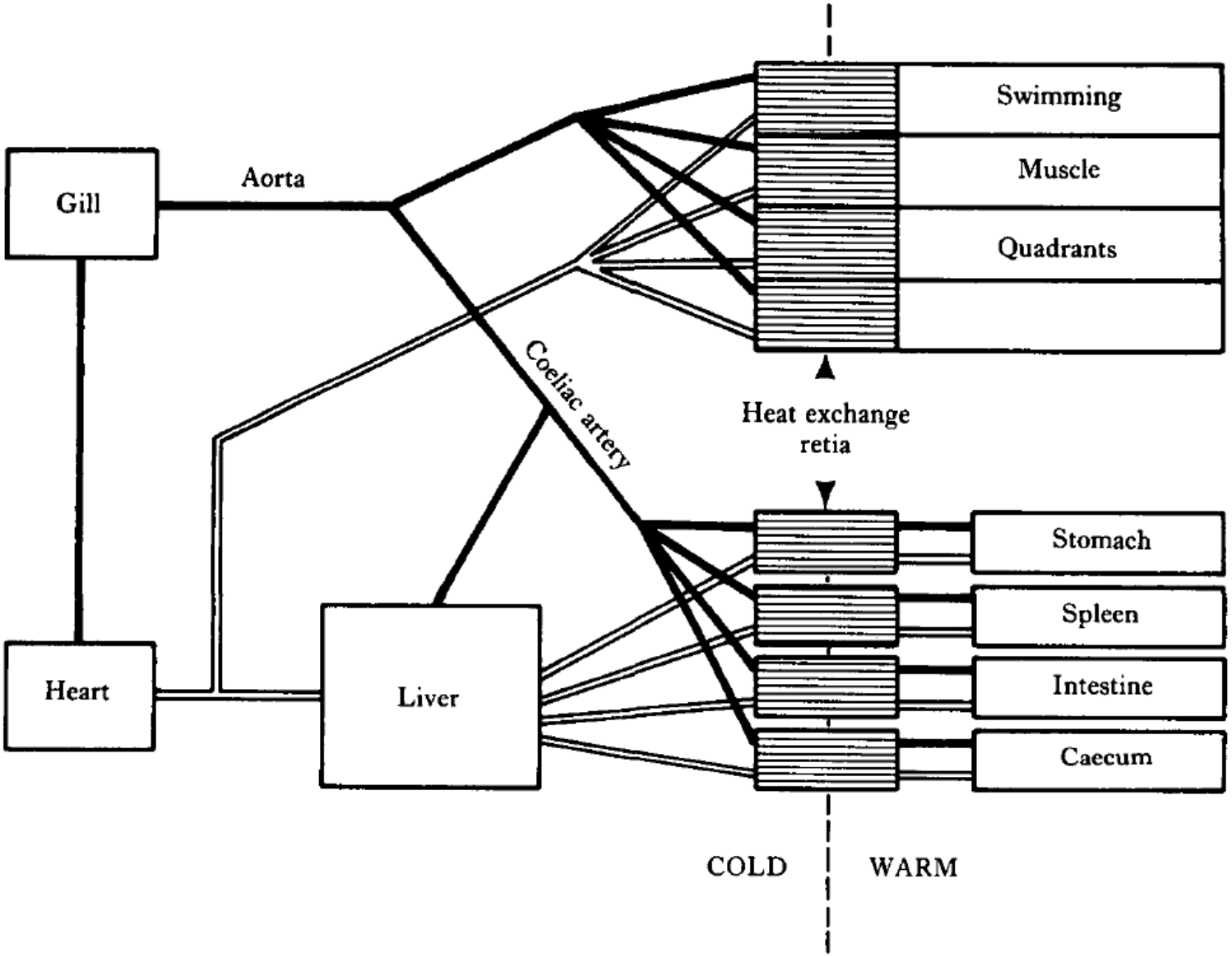

Fig. 10. Diagram of the circulatory system of a bluefin tuna. The heat exchange retia form a thermal barrier which prevents the blood from carrying heat away from the warm organs to be lost in the gills. Blood and tissue on the distal side of the rete is warm, that on the cardiac side is cool. Note that the heart and liver are on the cold side of the heat exchangers. Arteries, black; veins, white.

Carey et al. J. exp. Biol. 1984. 109, 1-20.

Wärmeaustauschsystem in Thunfisch

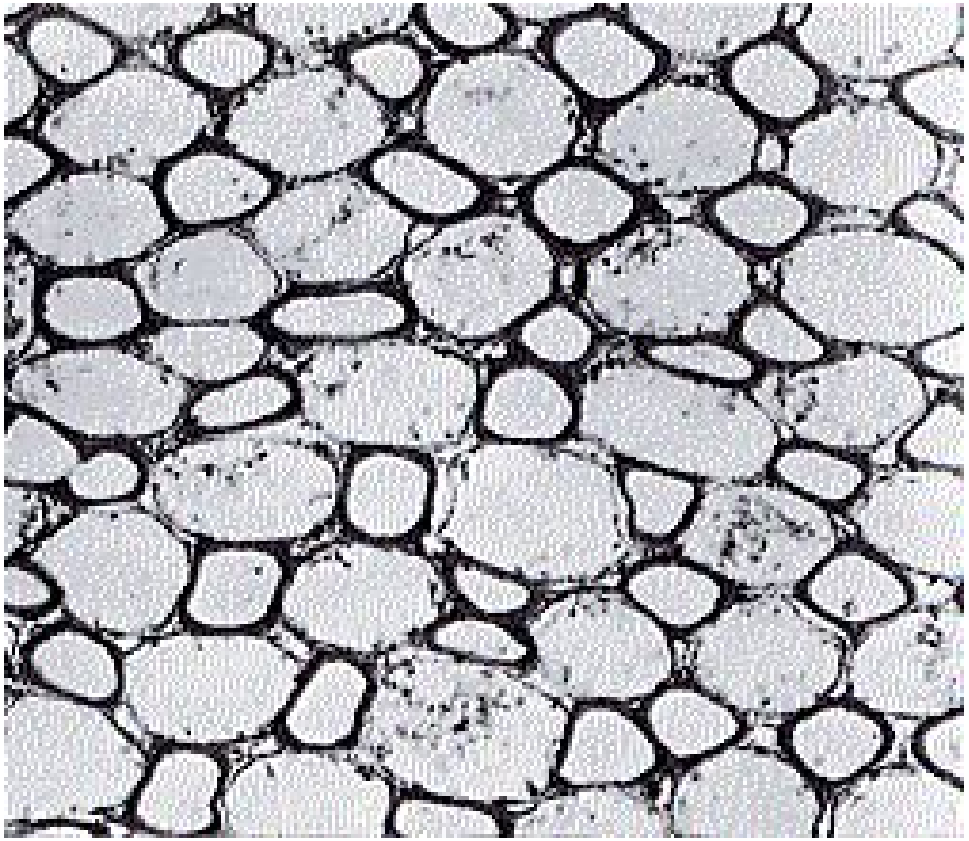

Histologie E.D: Stevens, Univ. Guelph, Canada)

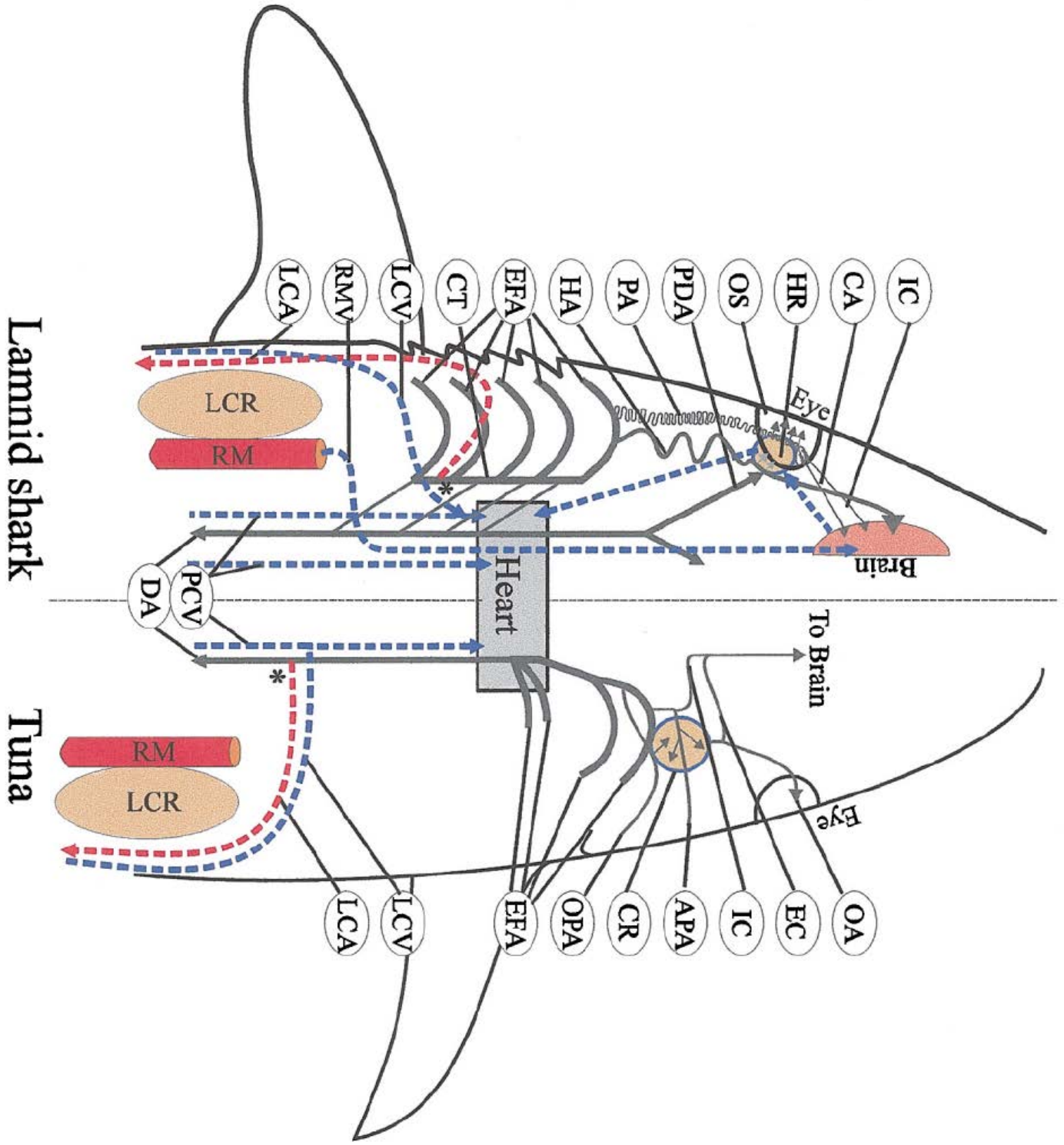

Fig. 8. Simplified comparative schematic showing vascular specializations for eye and brain endothermy in lamnid sharks and tunas. Arrows indicate the expected blood-flow direction in arteries (solid, gray) and veins (dashed, blue). Lamnid shark diagram is representative of *Isurus oxyrinchus* and *Carcharodon carcharias* and is missing the additional pseudobranchial *rete* present in both *Lamna* species (see Section 5.3 for details). Major differences between the lamnid shark and tuna vascular anatomy related to endothermy are: (1) unlike tunas, lamnids have a red muscle vein (RMV) that delivers warm blood to the brain and eyes; (2) the heat exchanging *retia* of lamnids lies in close proximity to the eye, in tunas it is relatively farther away; and (3) differences in the approximate point of origin (∗) of the lateral cutaneous arteries (dashed, red). Abbreviations: APA, afferent pseudobranchial artery; CA, cerebral artery; CR, carotid *rete*; CT, collecting trunks for the efferent branchial arteries; DA, dorsal aorta; EC, external carotid; EFA, efferent branchial arteries; HA, hyoidean artery; HR, hyoidean *rete*; IC, internal carotid; LCA, lateral cutaneous artery; LCR, lateral cutaneous *rete*; LCV, lateral cutaneous vein; OA, optic artery; OPA, opercular artery; OS, orbital sinus; PA, pseudobranchial artery; PCV, post cardinal vein; PDA, paired dorsal aorta; RM, red muscle. Modified from Linthicum and Carey (1972), Block and Carey (1985), Wolf et al. (1988), and Alexander (1998).

The vascular morphology and in vivo muscle temperatures of thresher sharks (Alopiidae)

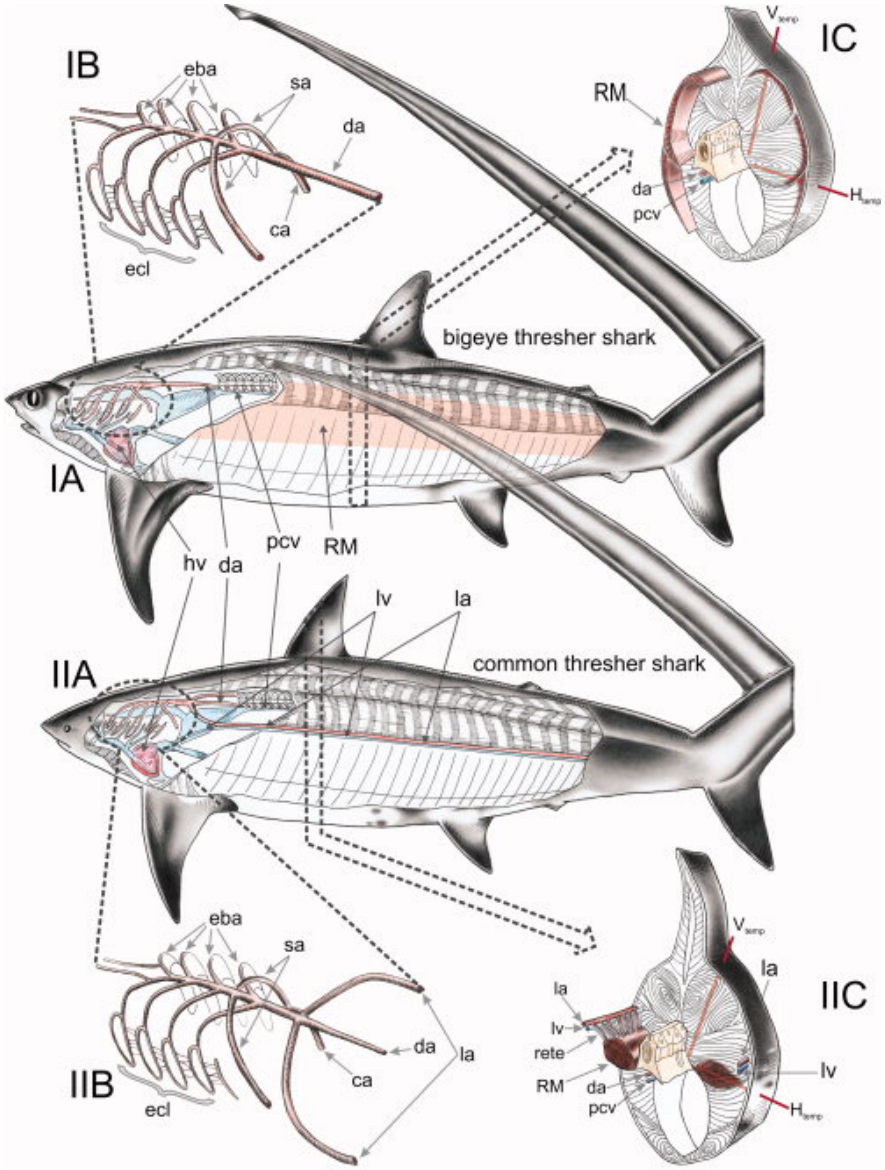

Journal of Morphology 17 JUN 2011 DOI: 10.1002/jmor.10989

The vascular morphology and in vivo muscle temperatures of thresher sharks (Alopiidae)

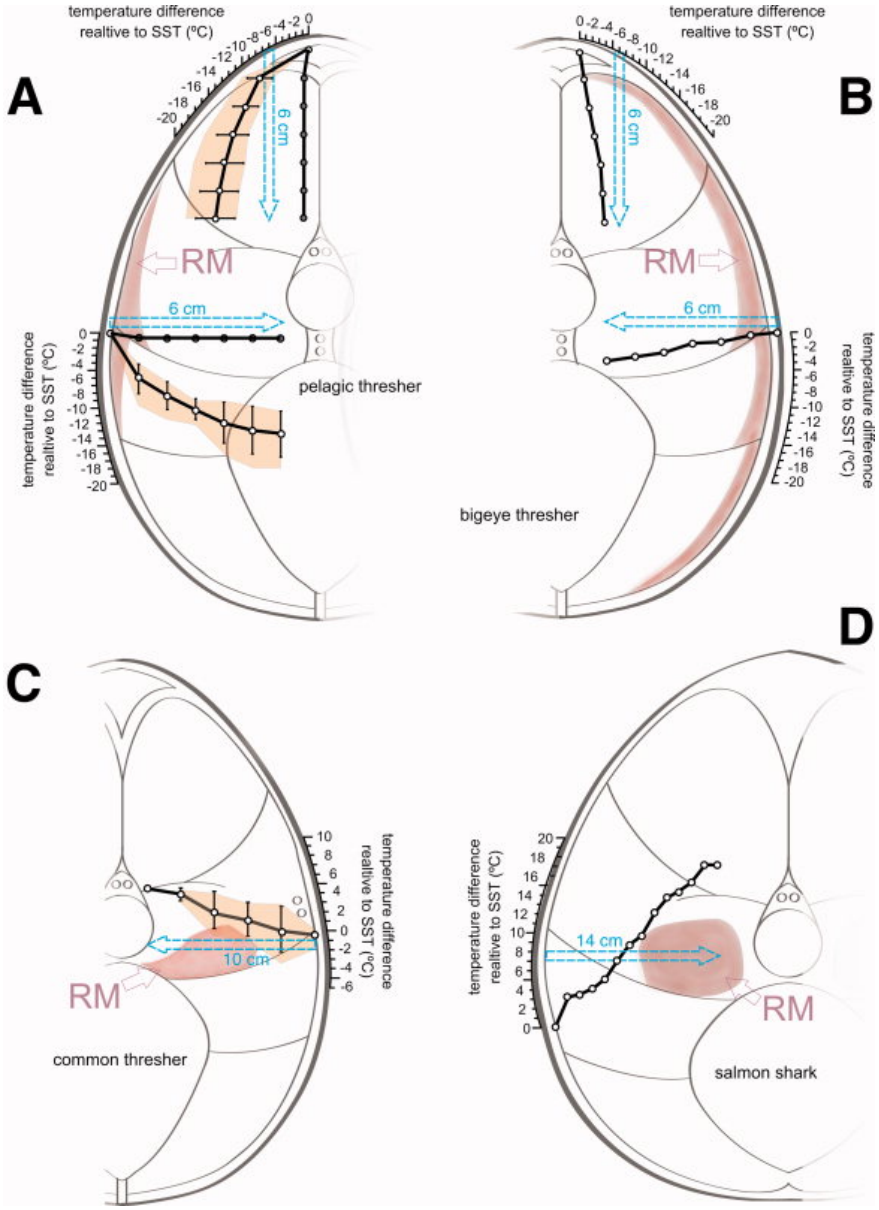

Journal of Morphology 17 JUN 2011 DOI: 10.1002/jmor.10989

Venenplexus zur Kühlung der Gonaden

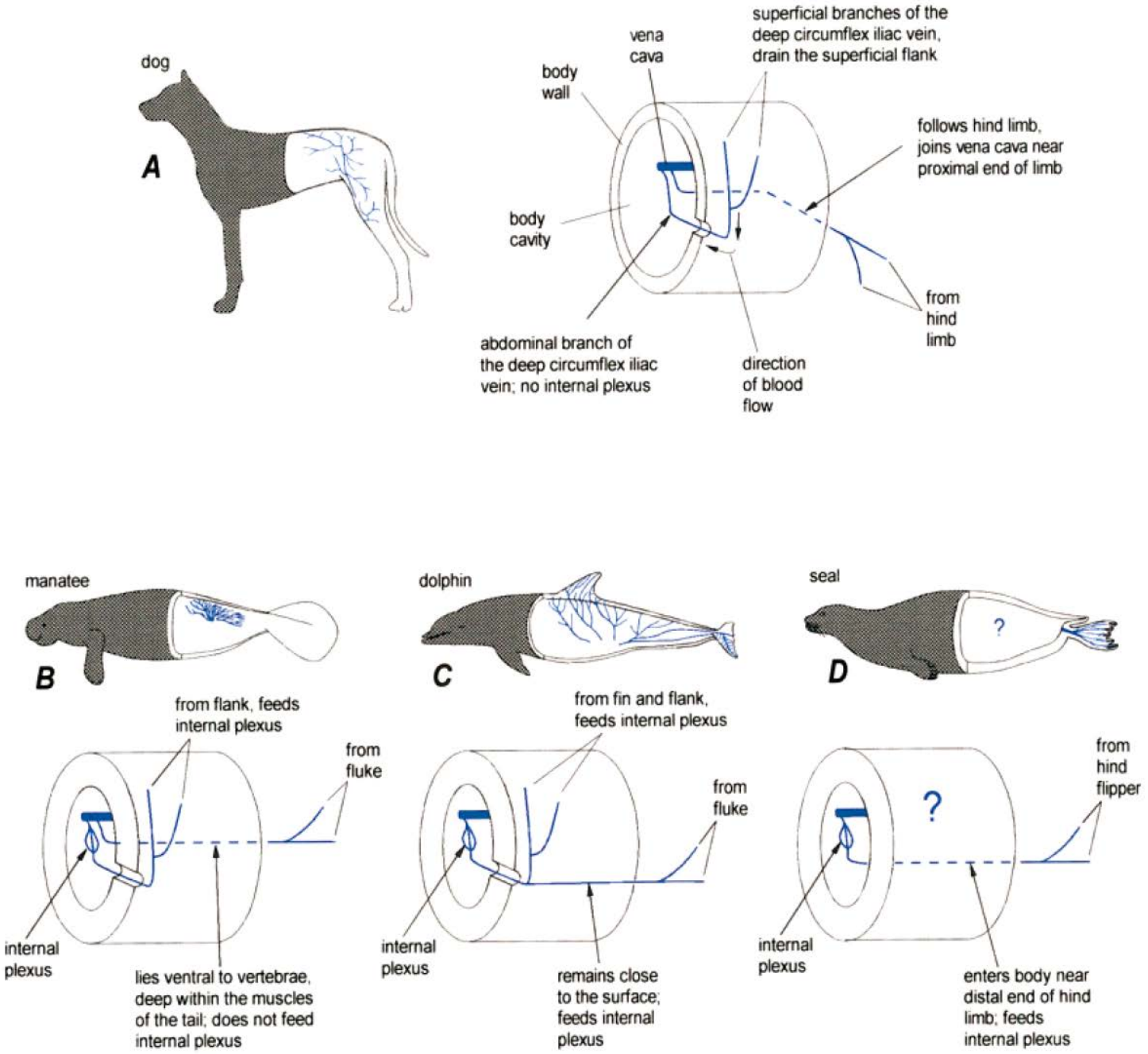

Rommel et al. 2001. Anatomical Record 264, 339-347.

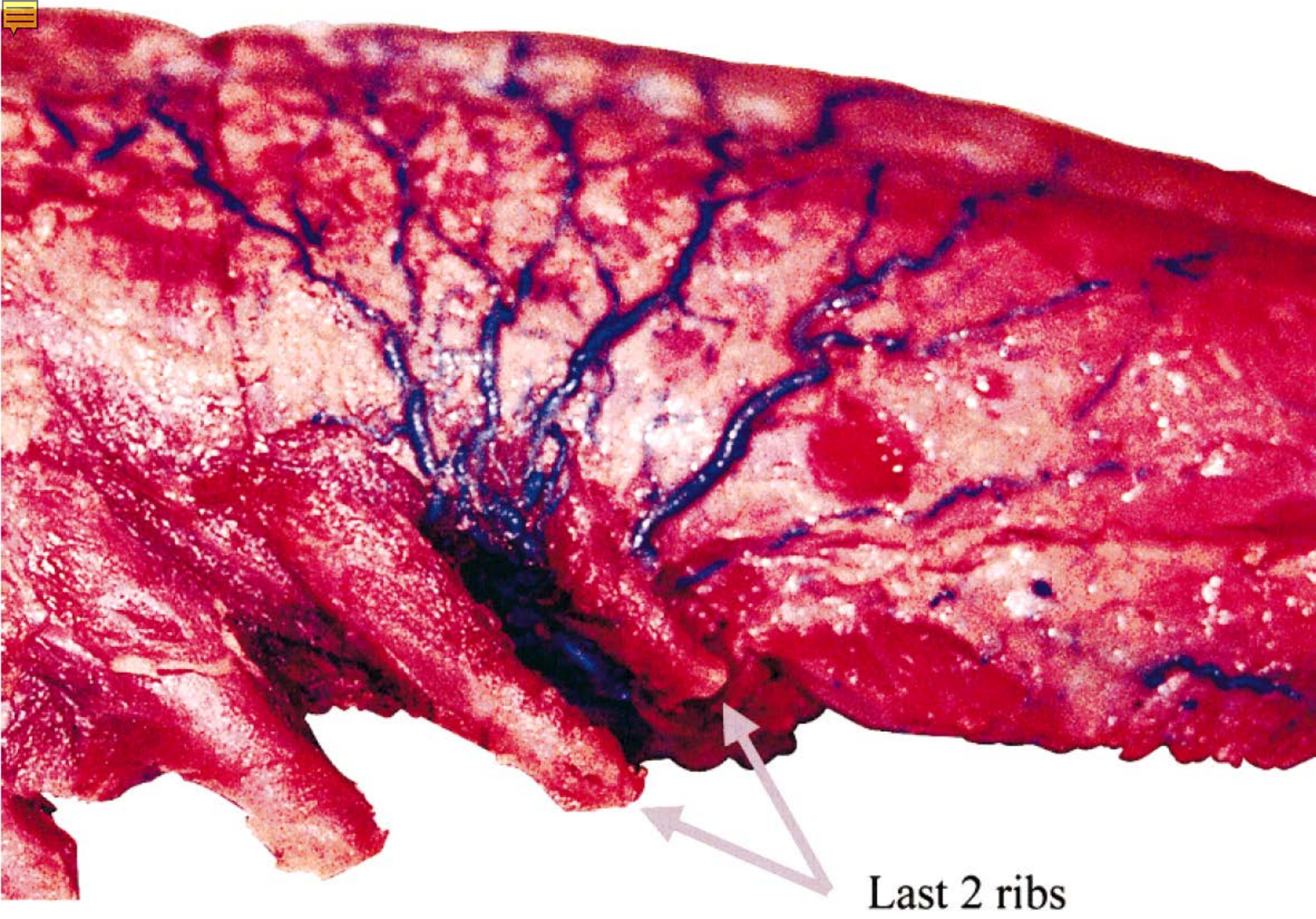

Rommel et al. 2001. Anatomical Record 264, 339-347.

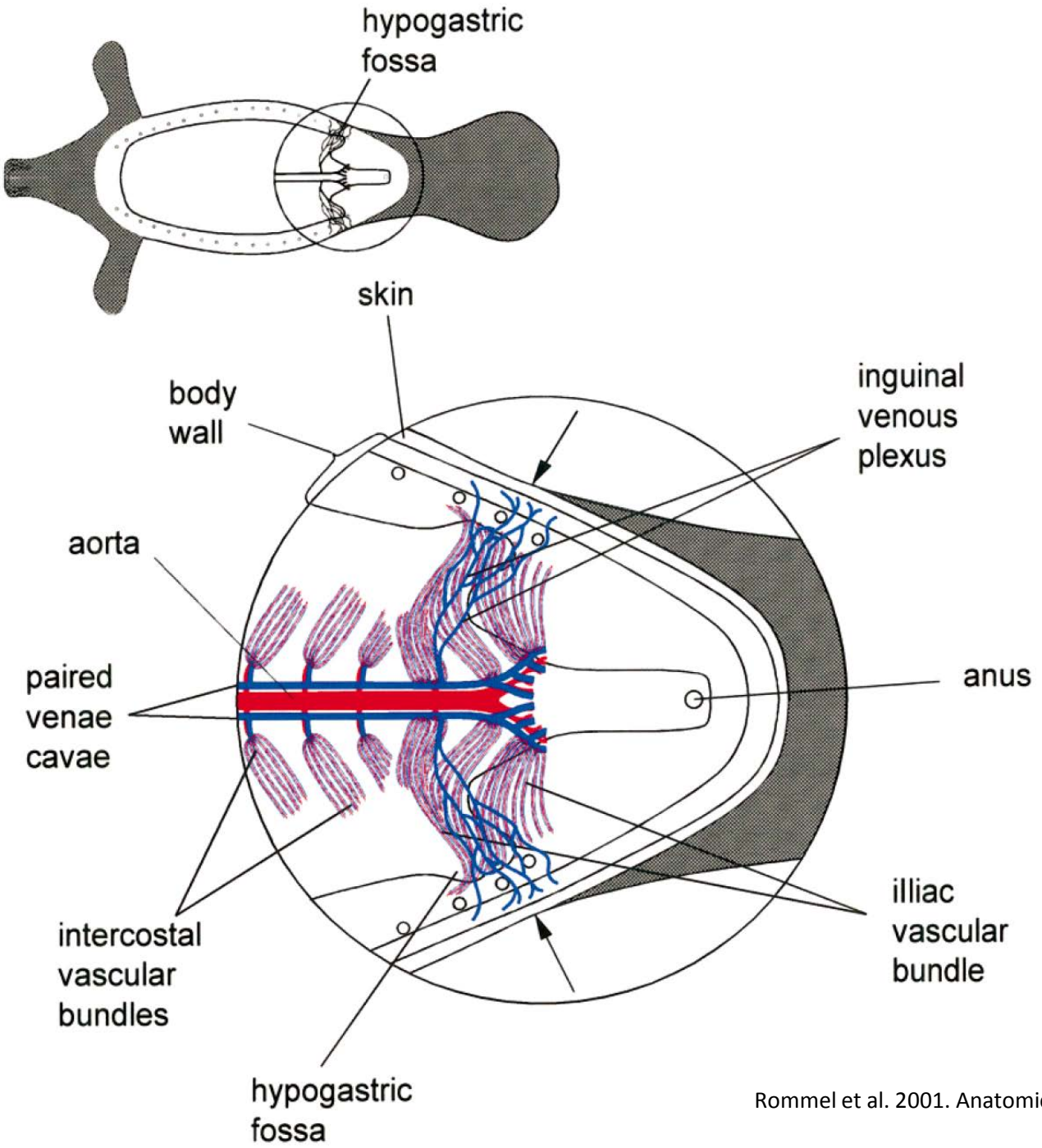

Rommel et al. 2001. Anatomical Record 264, 339-347.

Reproduktion

Temperaturabhängige Geschlechtsbestimmung bei Krokodilen

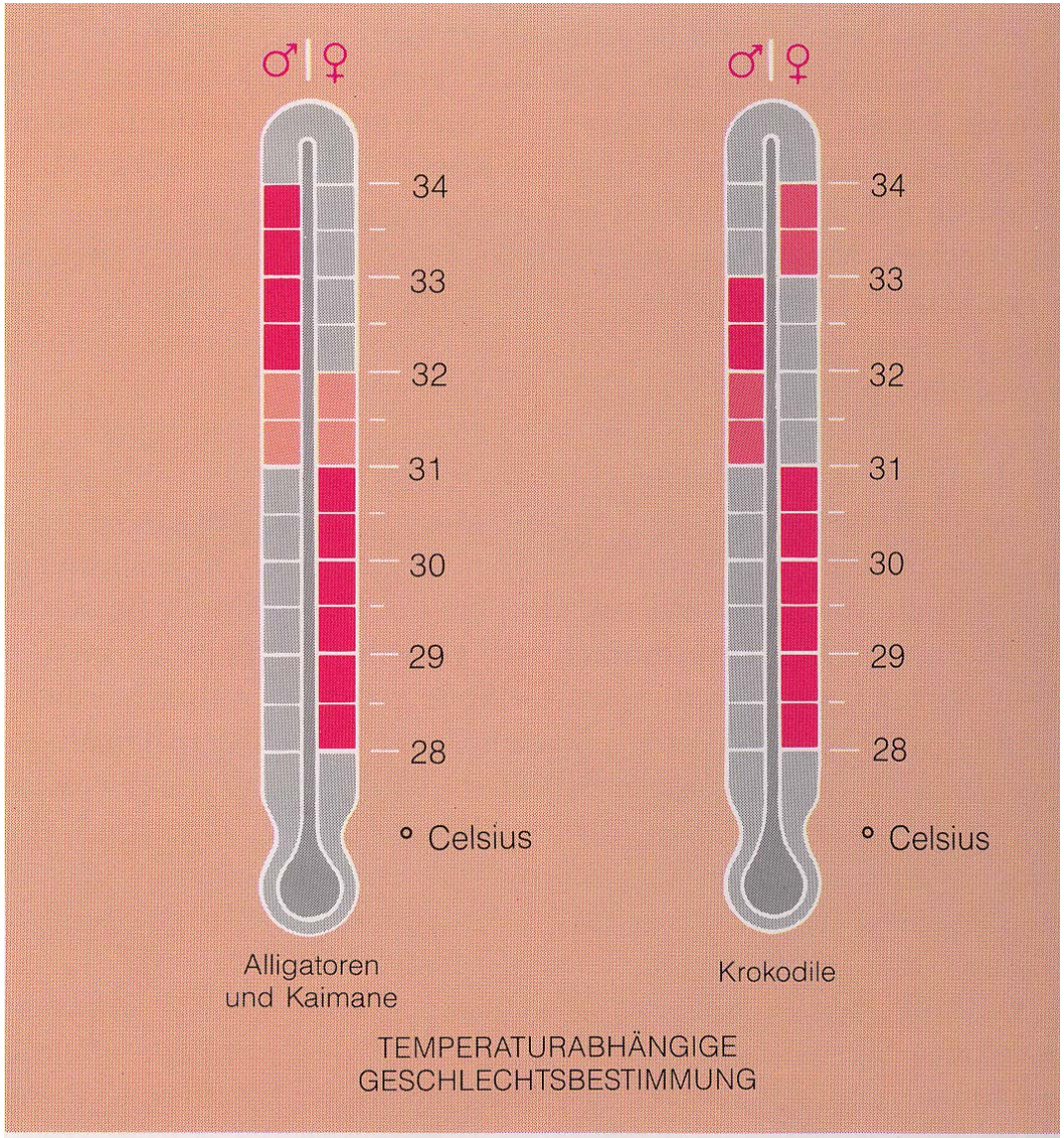

aus: Ross 2002. Krokodile und Alligatoren. Orbis Verlag, Niedernhausen

Temperature dependent sex determination

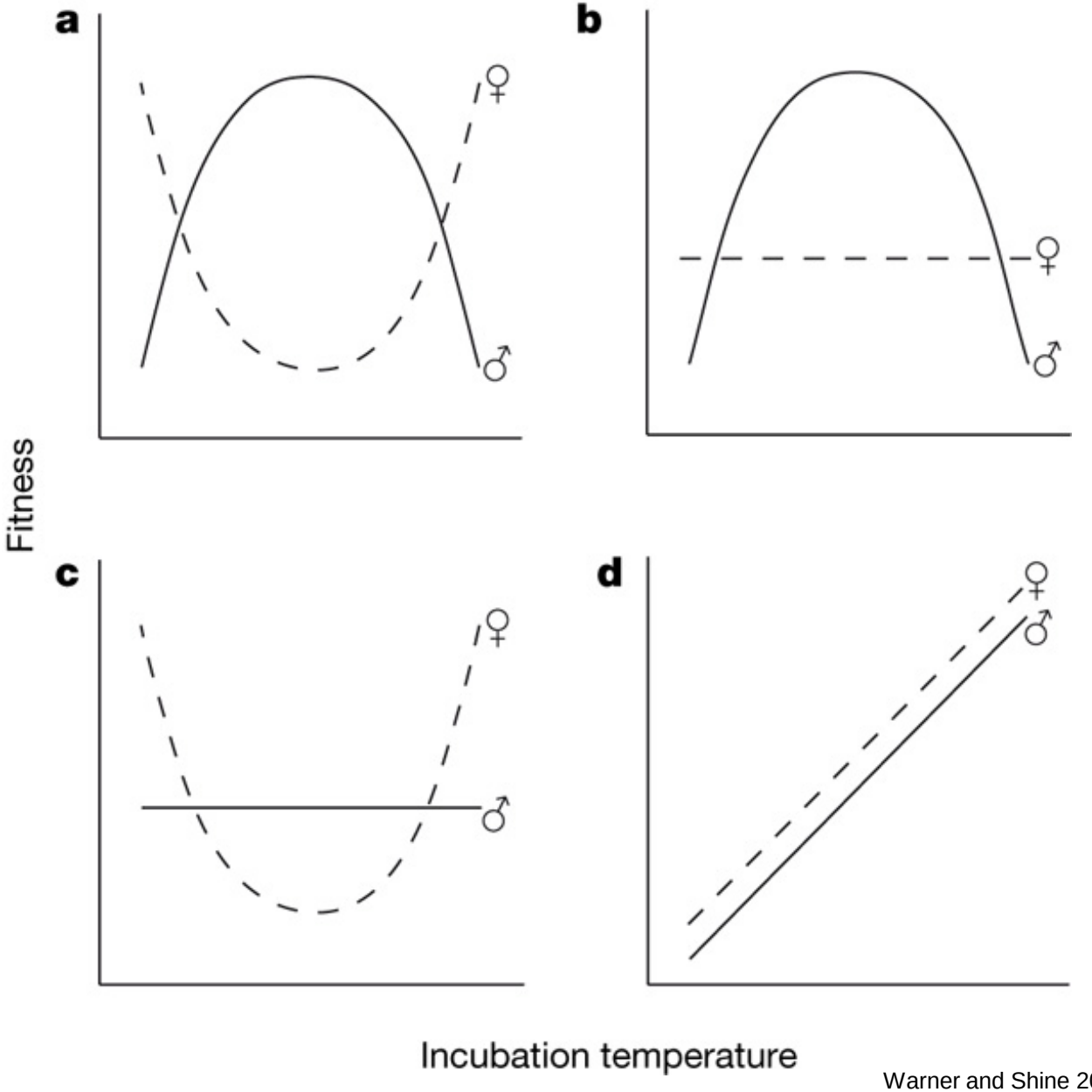

Warner and Shine 2008. *Nature* **451**, 566-568

TSD in *Amphibolurus muricatus*, Agamidae

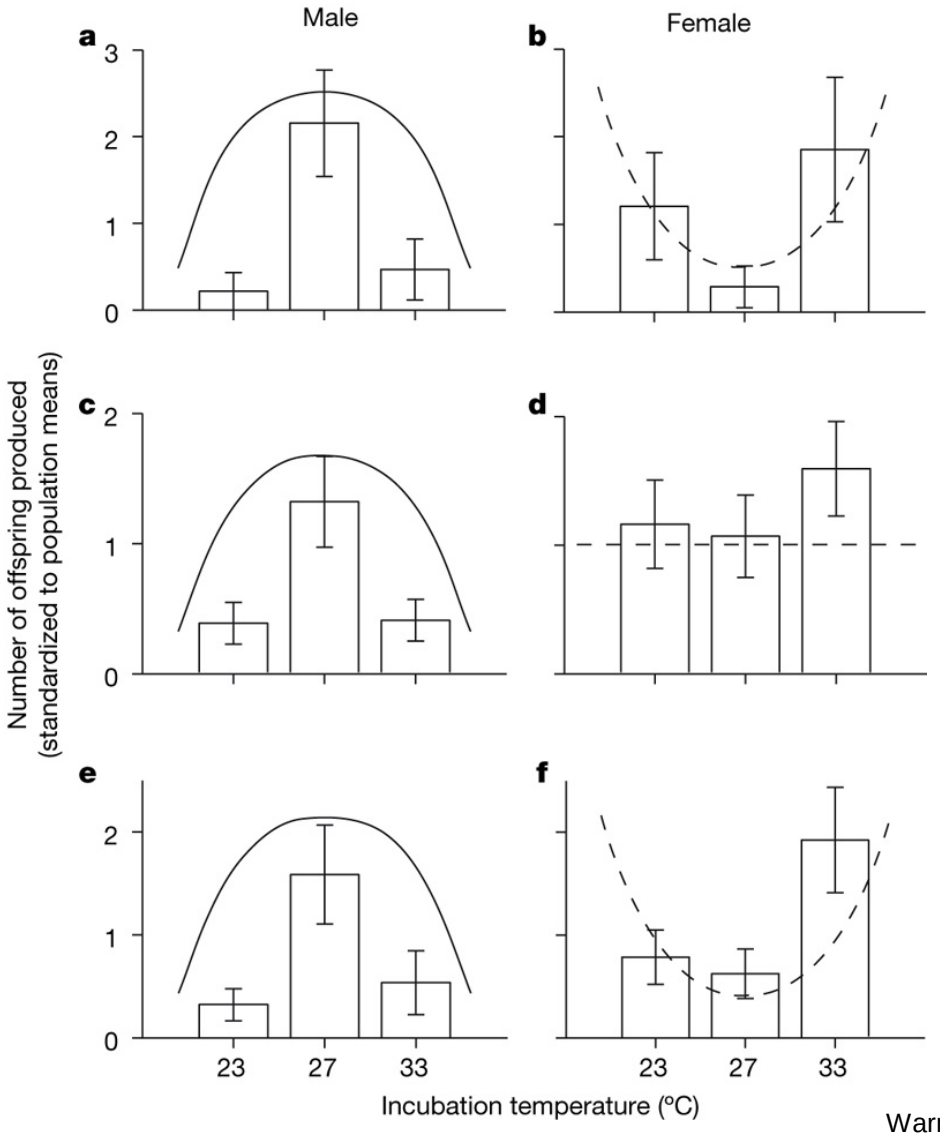

Warner and Shine 2008. *Nature* **451**, 566-568

Sex change in fish

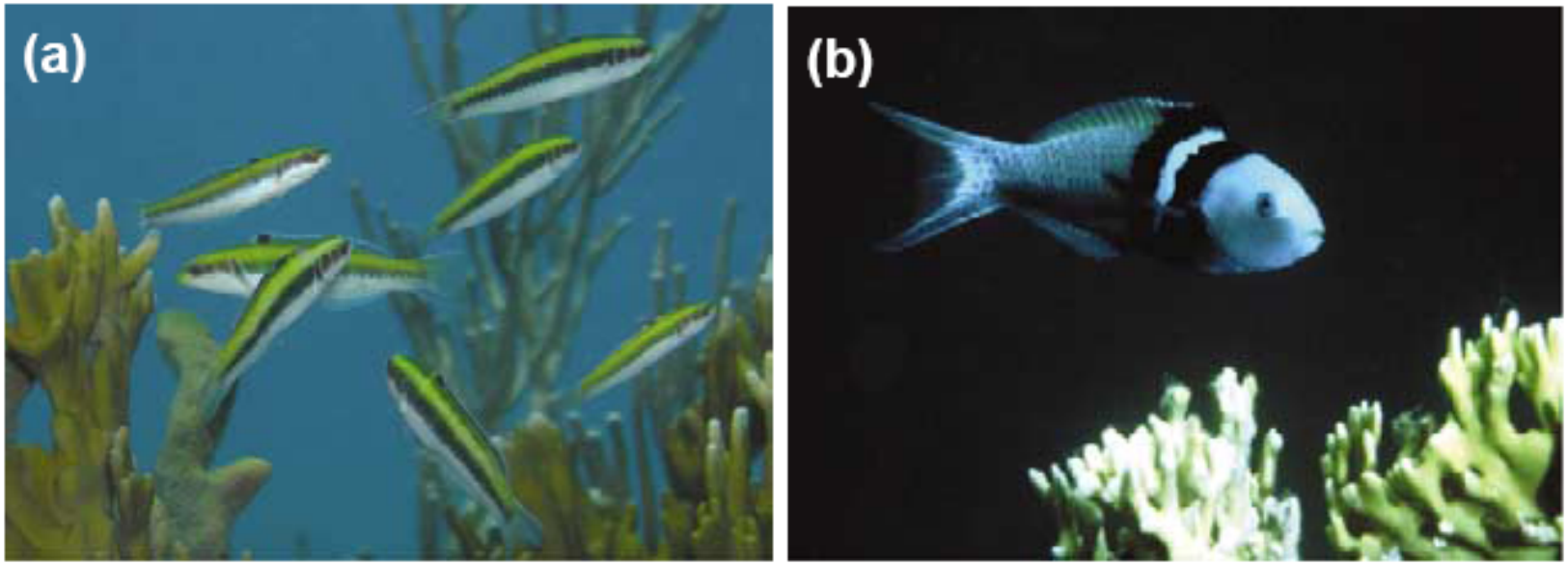

Figure I. Complex life histories of sex-changing animals. This is illustrated by the bluehead wrasse *Thalassoma bifasciatum* where individuals can mature as either a female or a primary male. Females and primary males look almost identical (**a**). Adult females change sex when they have the opportunity to take over the territory of a large male. Females that change sex and become a territorial male take on a distinct, bright colouration (**b**). Primary males can also become brightly coloured if they reach a size large enough to defend a territory, even though they have not changed sex. Photographs reproduced with permission from Will White and Ken Clifton.

Munday et al. 2006. TREE 21, 89 – 95.

Sex changing fish

Sex change in fish

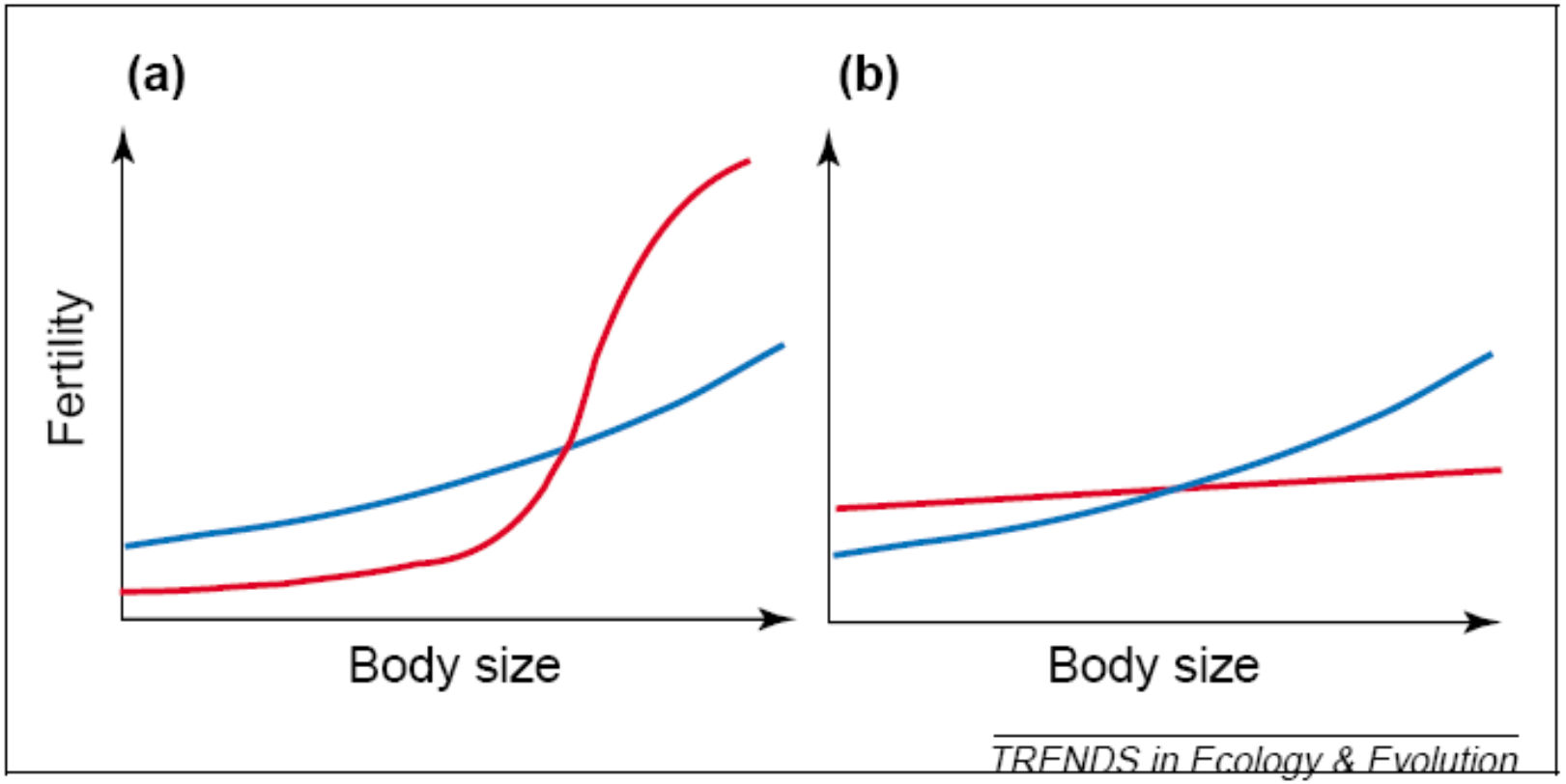

Munday et al. 2006. TREE 21, 89 – 95.

Nestflüchter und Nesthocker bei Vögeln

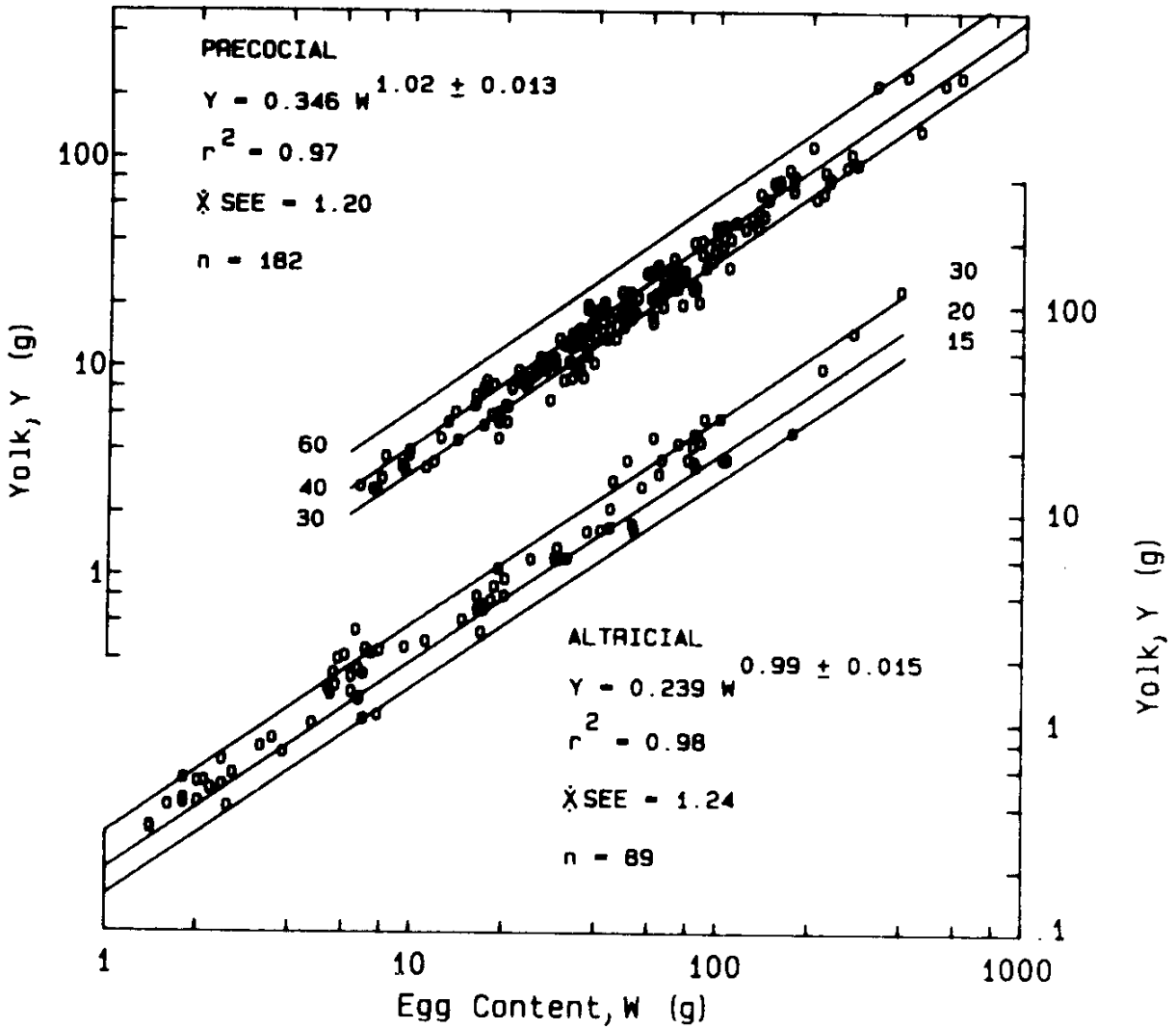

Figure 10.1 The relation between yolk mass (g) to mass of egg contents (g) in eggs of precocial (including all developmental categories of precocial, semiprecocial, and offshore and pelagic seabirds) and altricial (including semialtricial) species. The lines indicate isopleths for yolk as percent egg content from 15% to 60%. (Reprinted with permission from Sotherland and Rahn 1987).

from: Carey 1996. Female reproductive Energetics. In. Avian Energetics and Nutritional Ecology. (Cynthia Carey, ed.).Chapman and Hall, New York

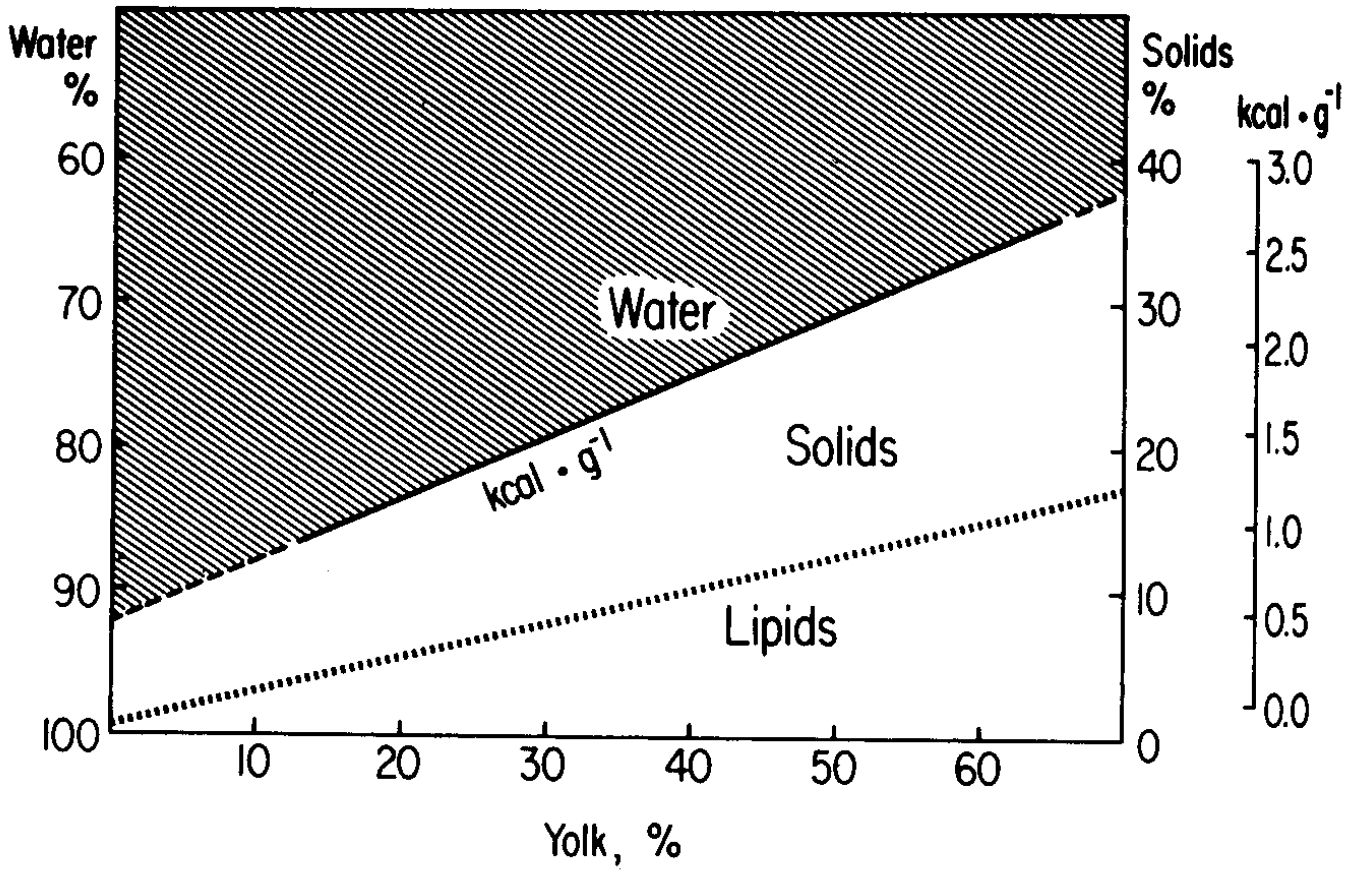

Figure 10.2 The relation between solids, water, and lipid as a function of varying yolk content (as percent of egg content) in avian eggs. The solid line represents the regression equation: dry egg content = 8.02 + 0.42 yolk content and the dotted line represents the regression equation: lipid content = 0.749 + 0.232 yolk content. If yolk content of an egg is known, the solid line may be used to predict an approximate caloric value (kcal·g^{-1} wet mass) using the ordinate on the right. (Reprinted with permission from Carey et al. 1980.

from: Carey 1996. Female reproductive Energetics. In. Avian Energetics and Nutritional Ecology. (Cynthia Carey, ed.).Chapman and Hall, New York

Megapodiidae – *Alectura lathami*

Macrocephalon maleo

Verbreitung Megapodiidae

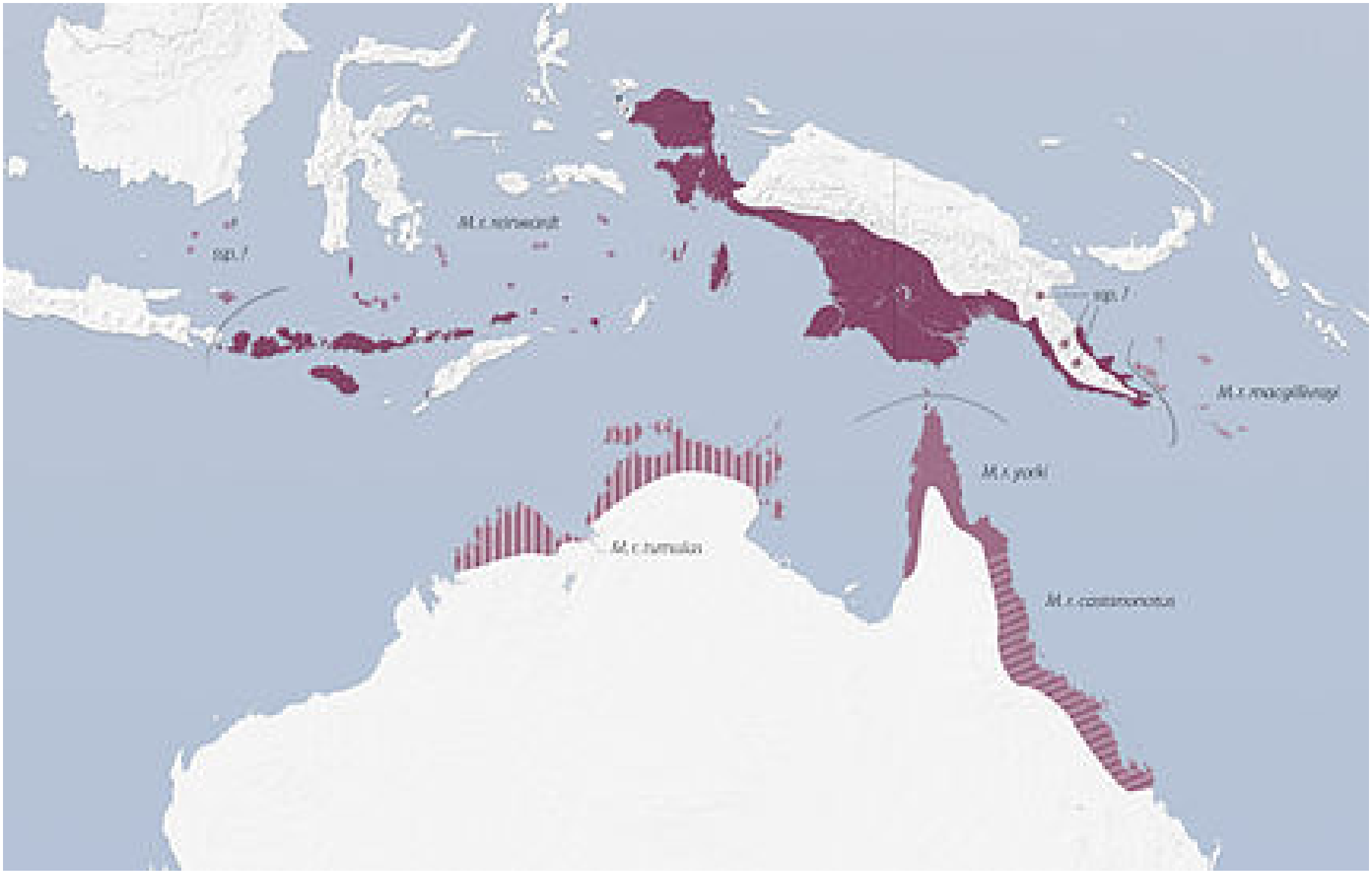

Macrocephalon Eier

Brutgebiet vulkanische Strände

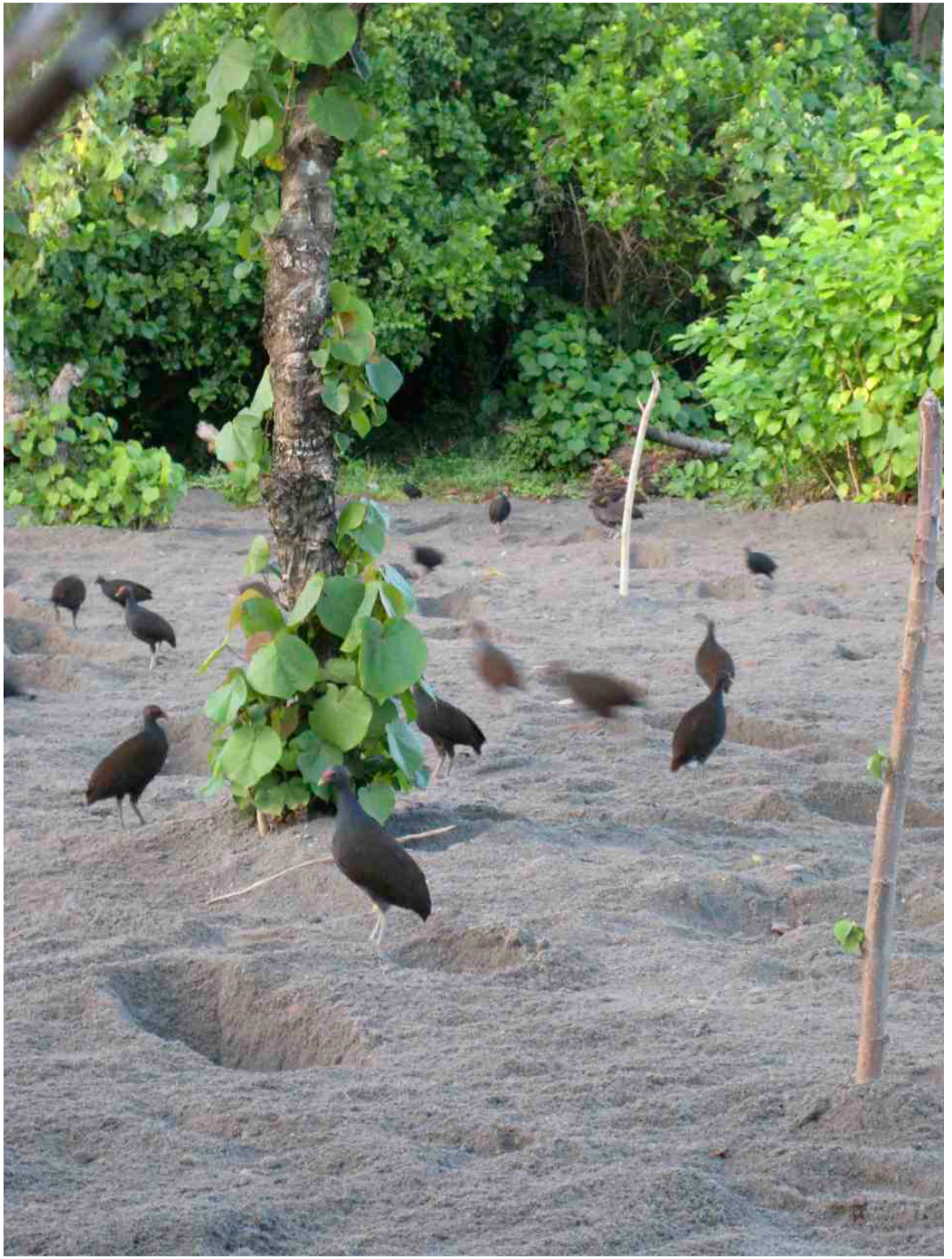

Megapodidae - Nestbau

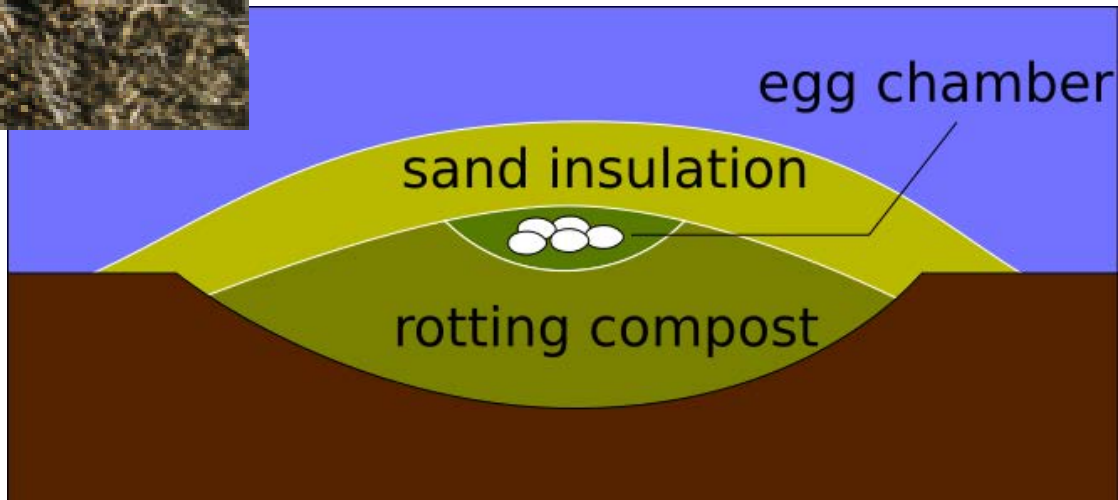

William E. Magnusson

▲ Da der Keilkopf-Glattstirnkaiman sein Nest im dichten Regenwald baut, kann er vom Sonnenlicht zur Regulierung der Nesttemperaturen keinen Gebrauch machen; stattdessen profitiert er von der Wärme, die von Termitenhügeln produziert wird. Die Eier werden in der Nähe des Hügels abgelegt, wo eine optimale Temperatur herrscht.

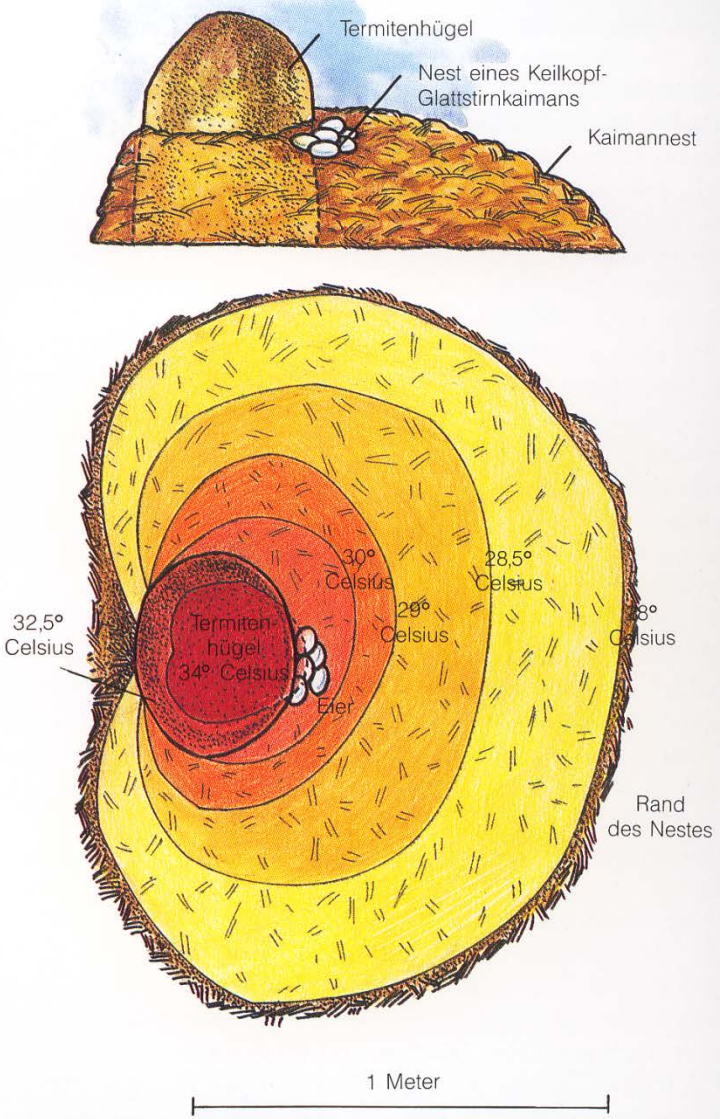

▲ Das Temperaturprofil durch ein Nest zeigt, wie die Stoffwechselwärme der Termiten hilft, die Temperaturen des Nestes zu erhalten. Das Zentrum des Termitenhügels ist mit 34 Grad Celsius möglicherweise zu heiß für die Eier, die Grenze des Nestes mit 28 Grad wahrscheinlich zu kühl. Aus diesem Grund wurden die Eier am Rand des Termitenhügels abgelegt, wo die Temperatur von 32 Grad für die Entwicklung der Jungtiere genau richtig ist.

aus: Ross 2002. Krokodile und Alligatoren. Orbis Verlag, Niedernhausen

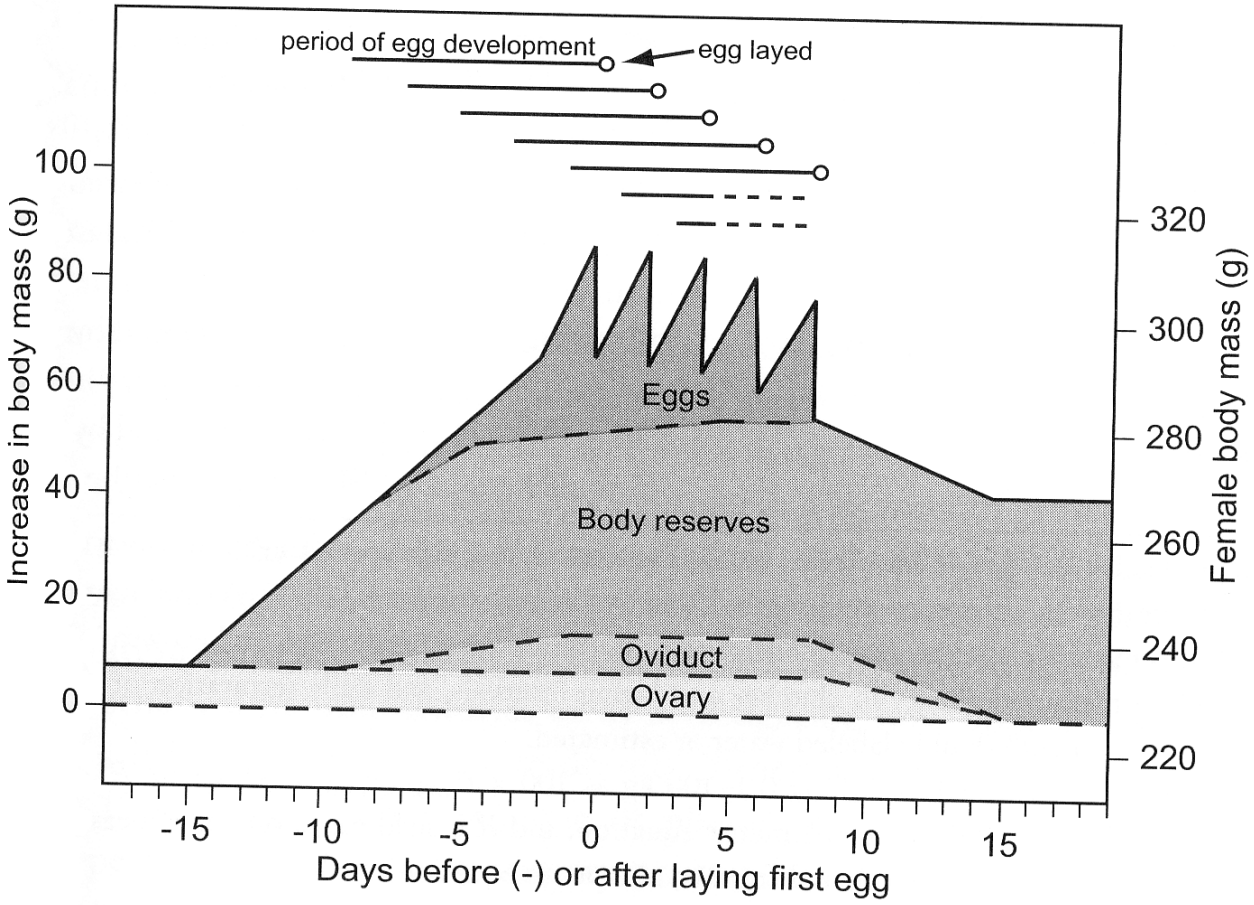

Figure 14.1. Female kestrels (*Falco tinnunculus*) build up body reserves before egg laying begins, and then during egg laying their day-to-day changes in body mass reflect the two day cycle from egg laying to deposition to egg laying. According to this model, the resources for egg laying do not come from the body reserves but from intake by the female. The reserves are used later, during the feeding of nestlings. (Redrawn from Meijer et al. 1989.)

from: Karasov and Martinez del Rio 2007. Physiological Ecology. Princeton UP.

Ca^{2+}-intake in egg laying female *Parus major*

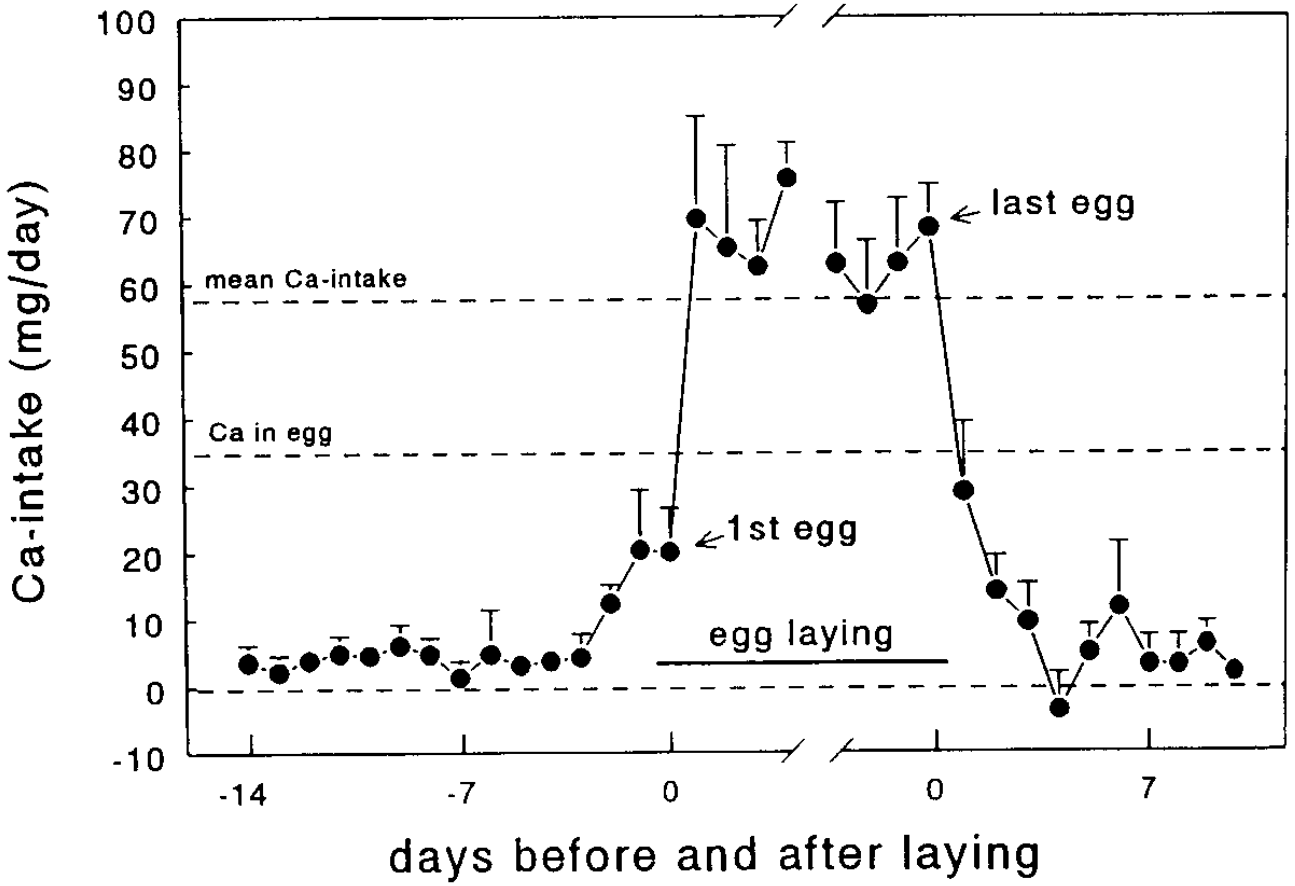

from: Carey 1996. Female reproductive Energetics. In. Avian Energetics and Nutritional Ecology. (Cynthia Carey, ed.).Chapman and Hall, New York

Figure 14.2. In kestrels (*Falco tinnunculus*), the time males spend hunting per day (figure A) and their daily energy expenditure (figure B) increased when brood size was experimentally changed from the natural mean of 5 young/brood. Data are from Dijkstra et al. (1990) and Deerenberg et al. (1995).

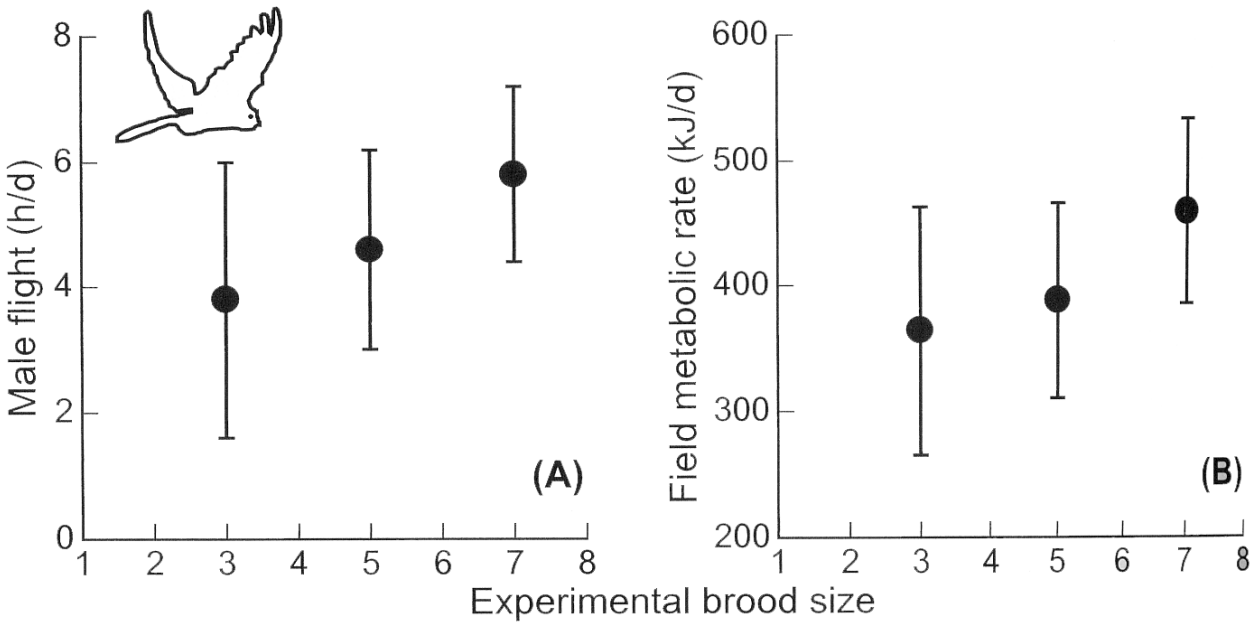

from: Karasov and Martinez del Rio 2007. Physiological Ecology. Princeton UP.

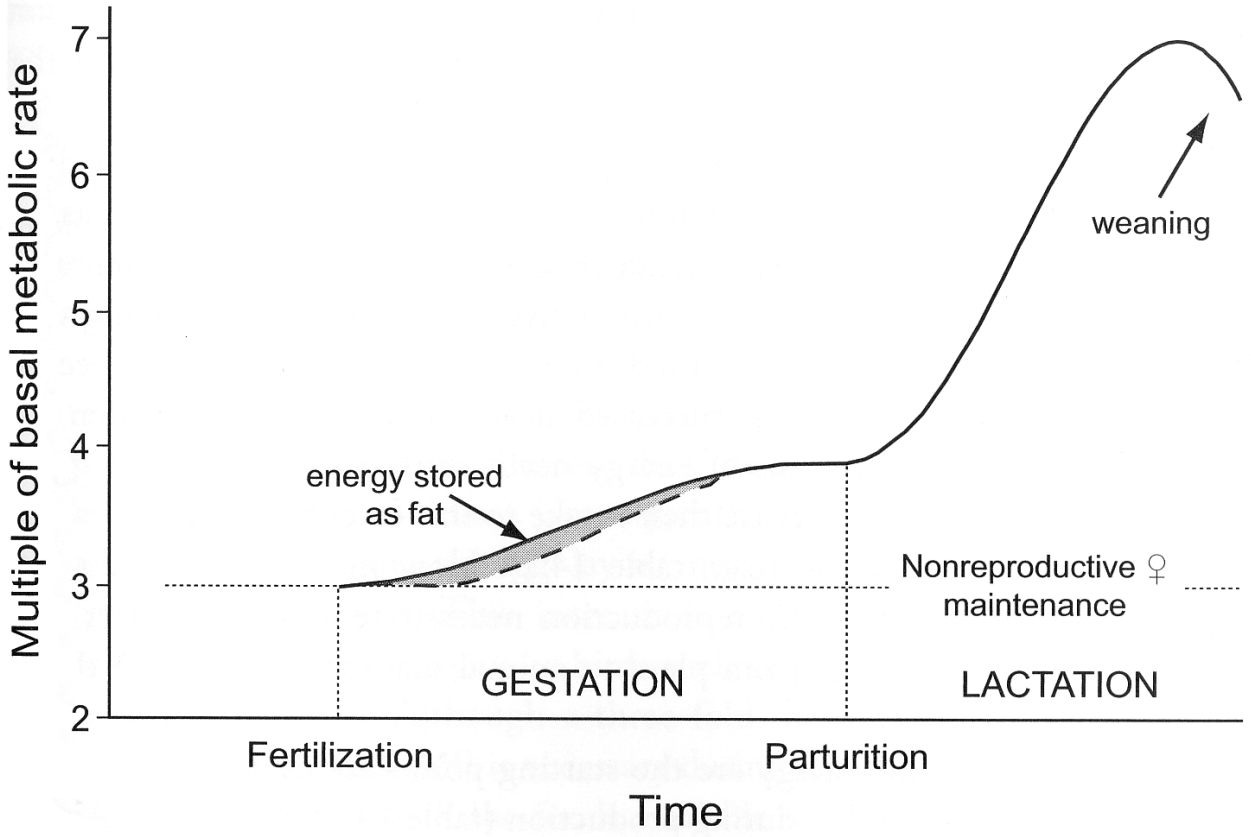

Figure 14.3. Typical pattern of metabolizable energy intake for small mammals during gestation and lactation. According to the model, nonreproductive females typically have energy intake and expenditures of around 3 times basal metabolic rate, and this increases <33% during gestation but >100% at peak lactation. The model shows that during gestation the intake may exceed the sum of respiration + allocation to reproductive tissue, with the difference being stored as fat. This fat store may or may not be used during lactation. (Redrawn from Thompson 1992.)

from: Karasov and Martinez del Rio 2007. Physiological Ecology. Princeton UP.

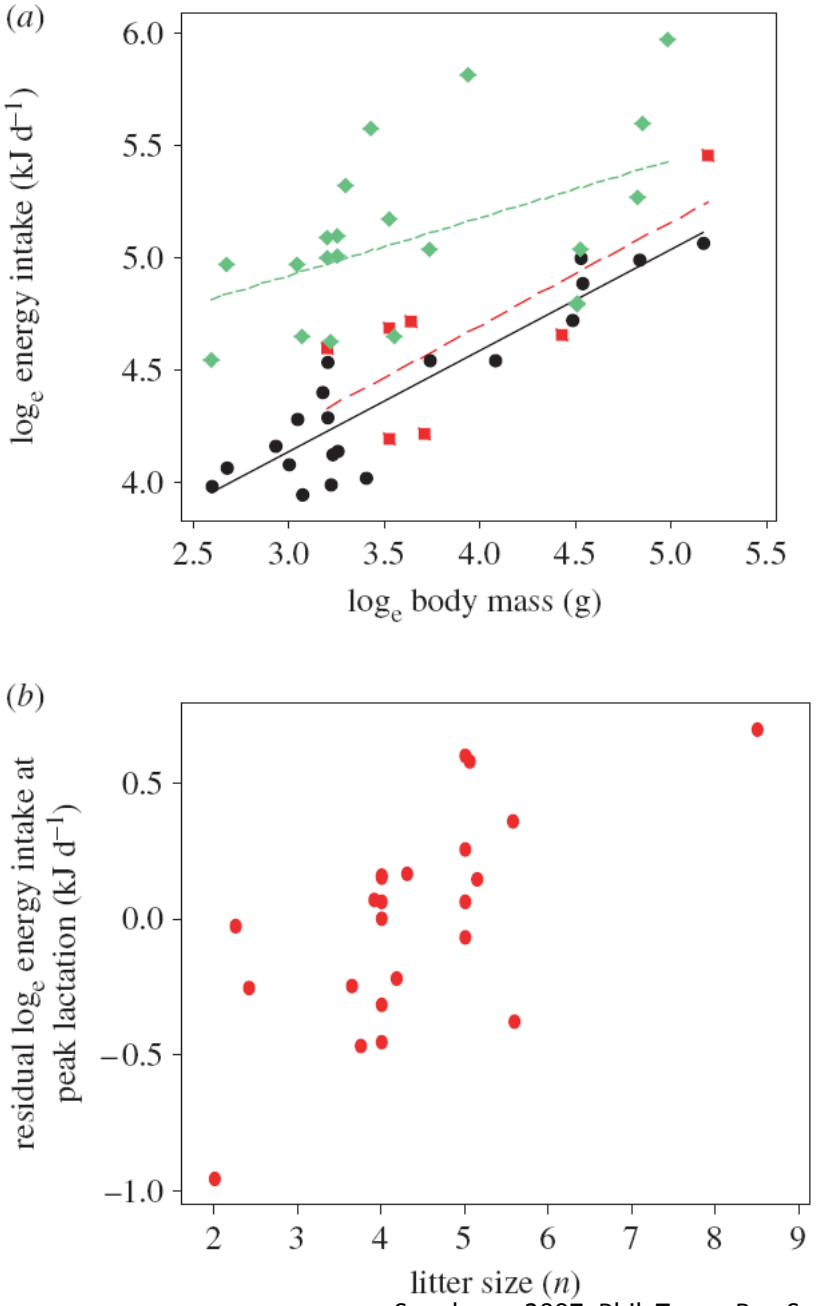

Speakman 2007. Phil. Trans. Roy Soc. London B. doi:10.1098/rstb.2007.2145

Food intake each day throughout pre-breeding, pregnancy and lactation phases for MF1 mice.

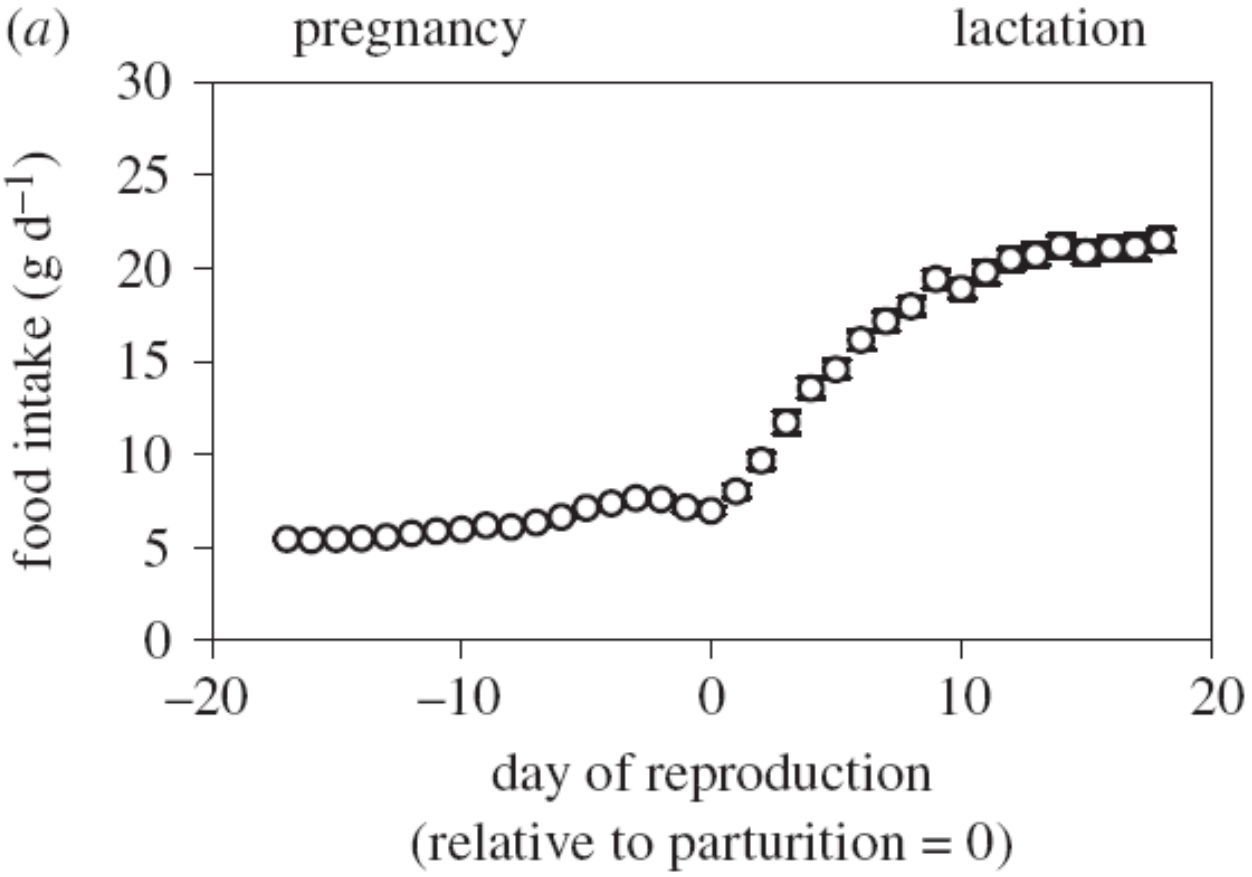

Speakman 2007. Phil. Trans. Roy Soc. London B. doi:10.1098/rstb.2007.2145

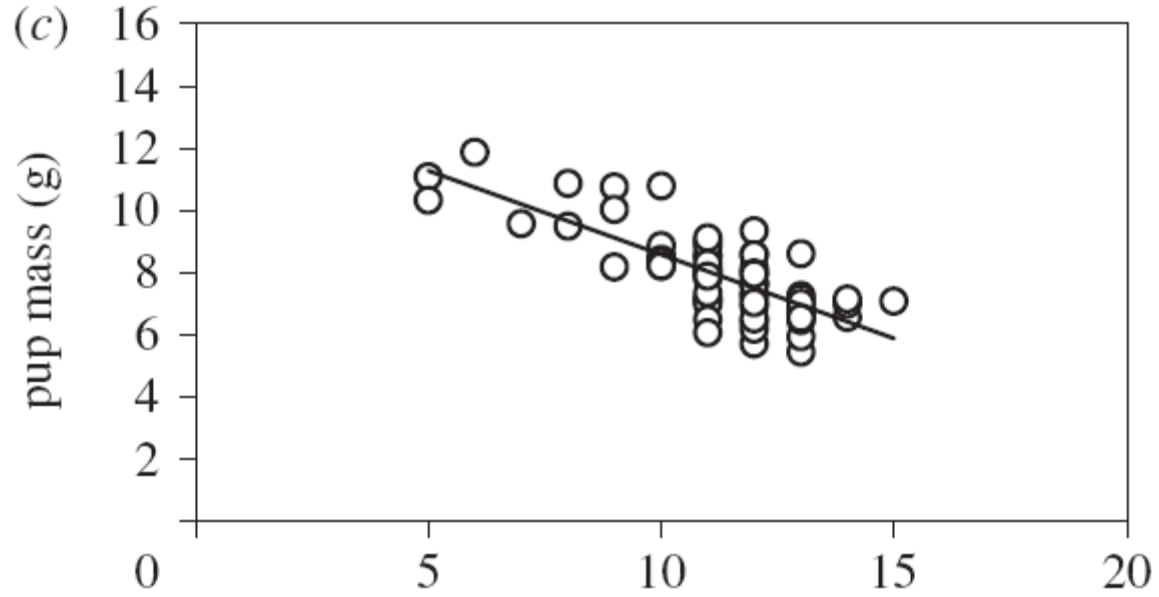

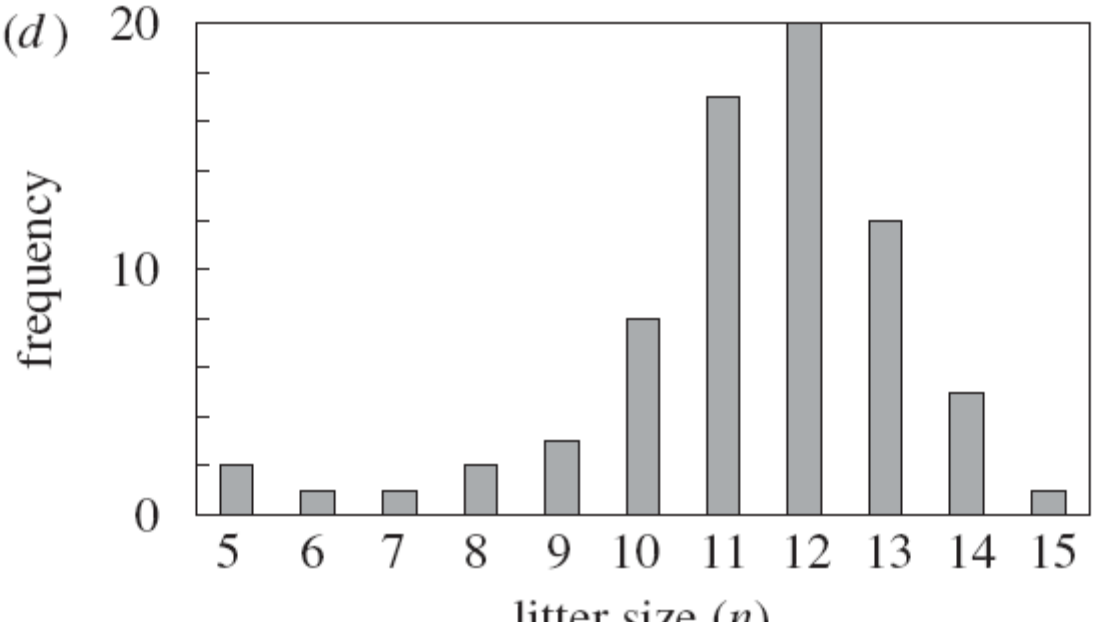

Speakman 2007. Phil. Trans. Roy Soc. London B. doi:10.1098/rstb.2007.2145

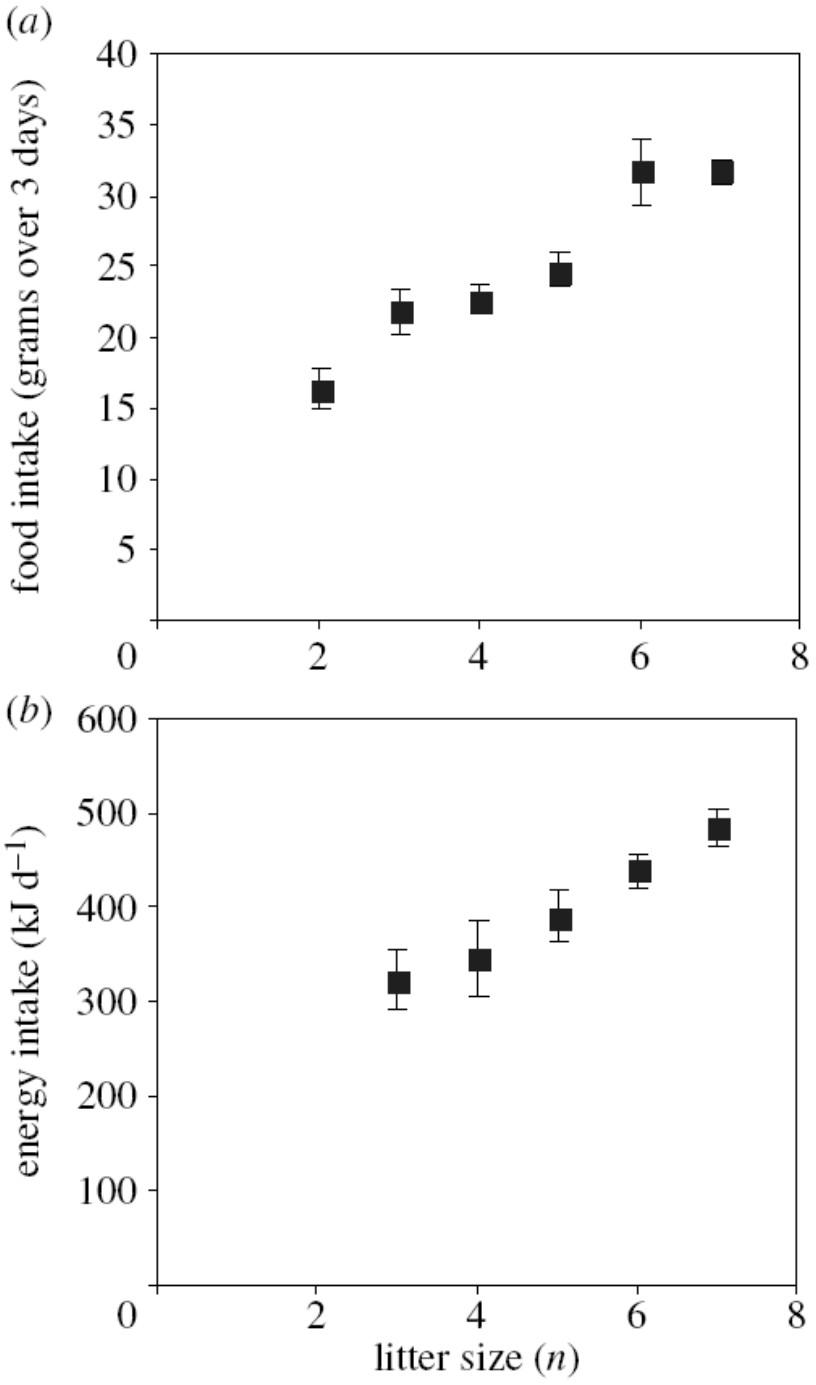

Figure 3. (*a*) Food intake at peak lactation (grams over 3 days) in relation to litter size in *Peromyscus leucopus* (drawn from tabulated data in Millar 1978). (*b*) Energy intake during lactation (kJ d^{-1}) in relation to litter size in *Sigmodon hispidus* (drawn from tabulated data in Rogowitz 1998).

Speakman 2007. Phil. Trans. Roy Soc. London B. doi:10.1098/rstb.2007.2145

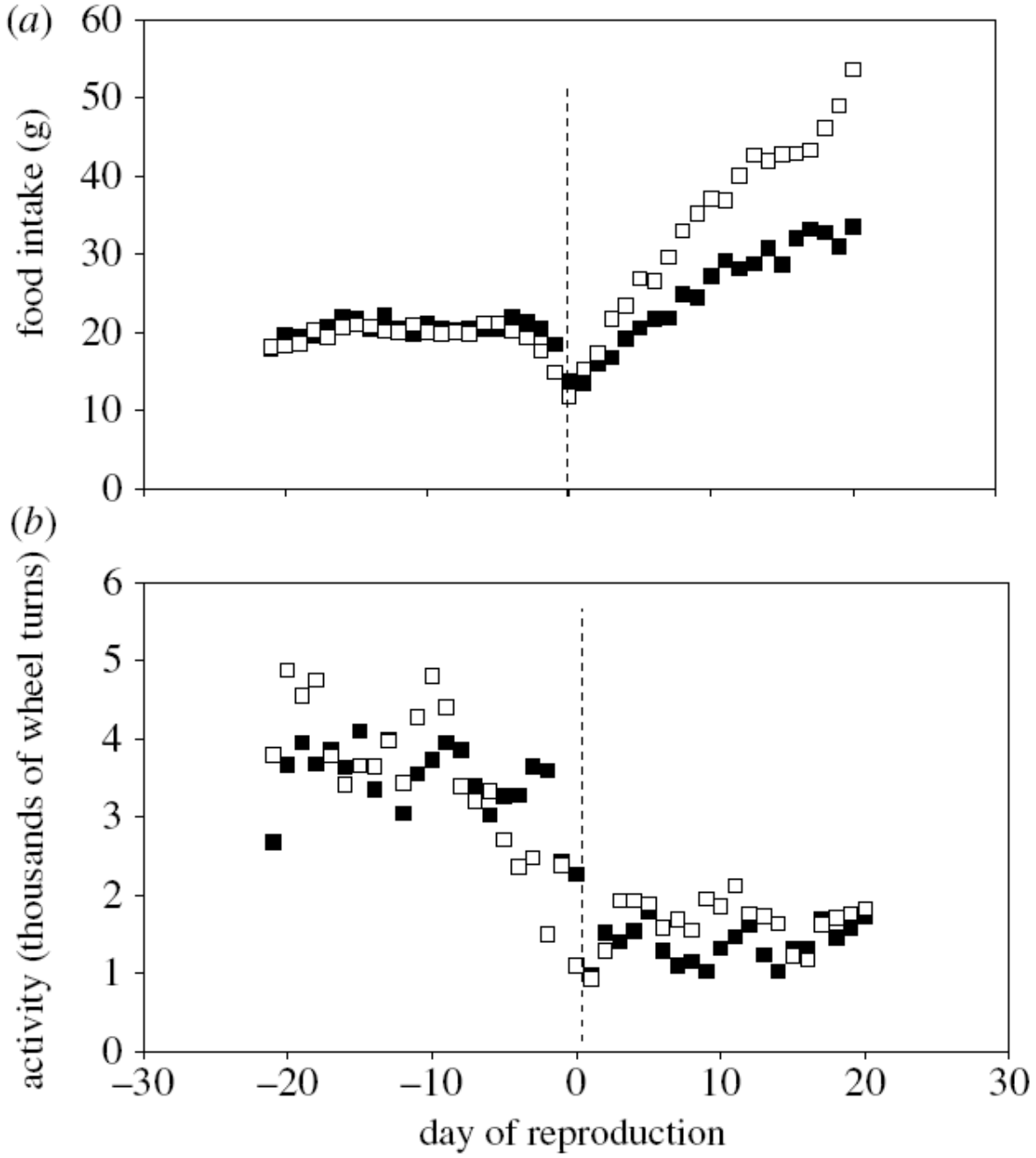

Speakman 2007. Phil. Trans. Roy Soc. London B. doi:10.1098/rstb.2007.2145

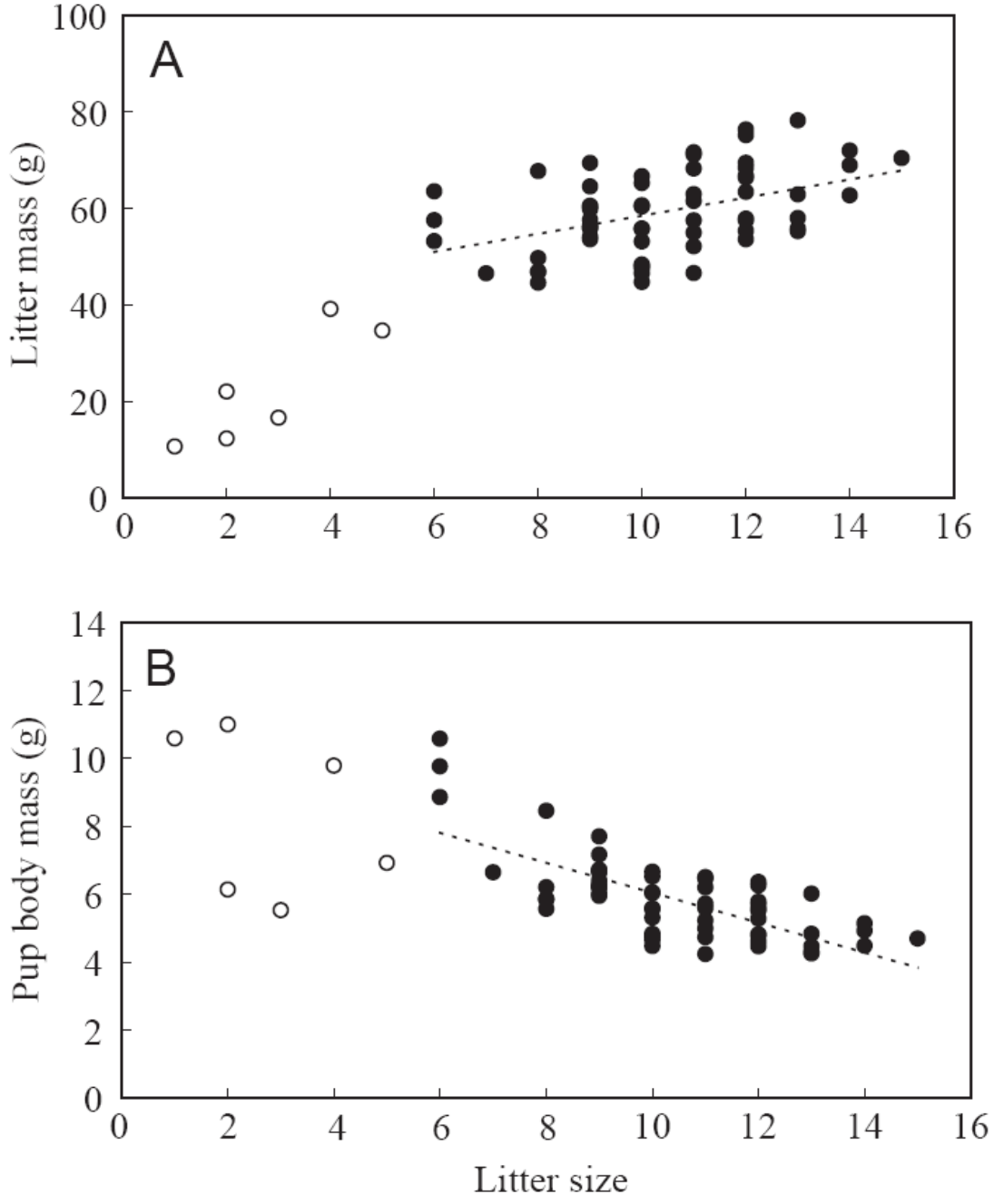
A
Litter mass (g)
0
20
40
60
80
100
0
2
4
6
8
10
12
14
16
B
Pup body mass (g)
0
2
4
6
8
10
12
14
Litter size

Metabolic ceilings

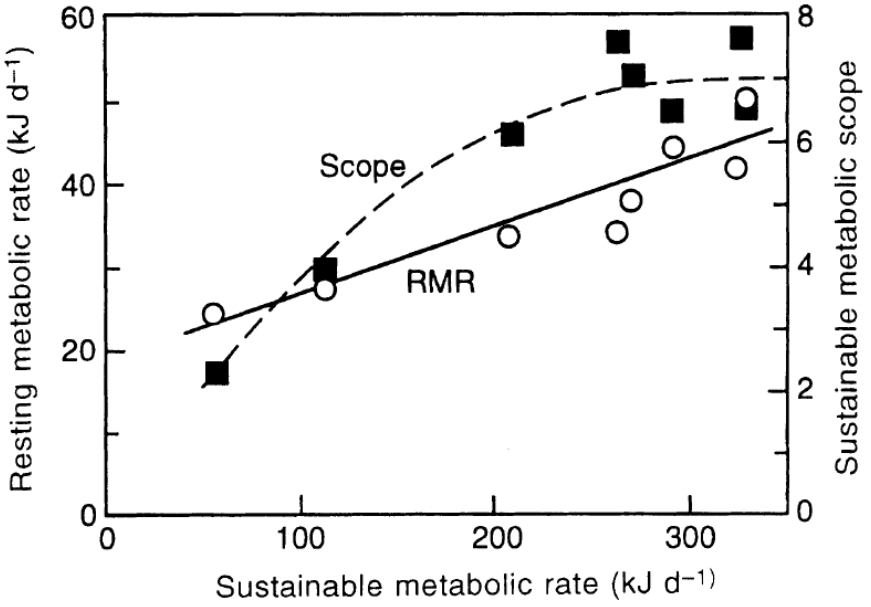

Figure 1 Measured or estimated values of RMR, and calculated values of SusMS (metabolic scope), in female mice, plotted as a function of SusMR. SusMR was manipulated experimentally by applying cold stress, lactation with various litter sizes from 5 to 14 pups, or cold stress plus lactation. The left-most point is for virgin mice at 23 °C; the right-most point, for mice nursing 14 pups at 5 °C. Note that both RMR and SusMS increase with SusMR. The straight line through RMR values, and the curve fitted by eye through SusMS values, serve merely to summarize trends and have no theoretical significance. Data are from ref. 8 and our unpublished measurements.

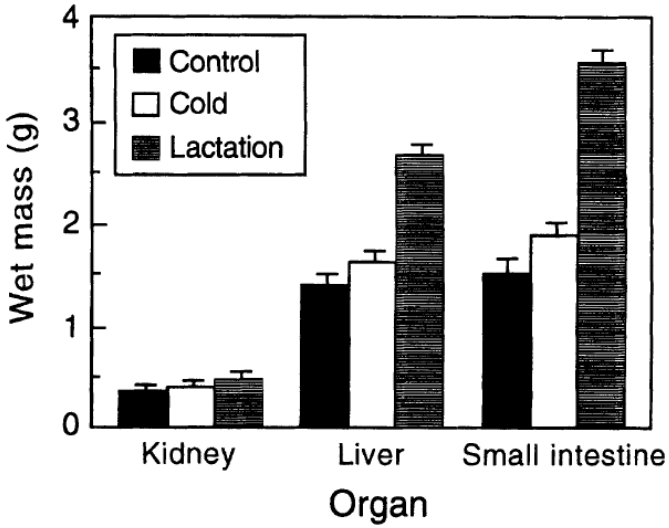

Figure 2 Changes in wet mass of kidney, liver and small intestine in mice with three increasing levels of energy demand (from left to right: control or virgin females, acclimation to 5 °C, and lactation with a litter of 8 pups). Within each organ, changes of organ mass with energy demand are statistically significant at $P < 0.05$ by ANOVA. Data are from ref. 8.

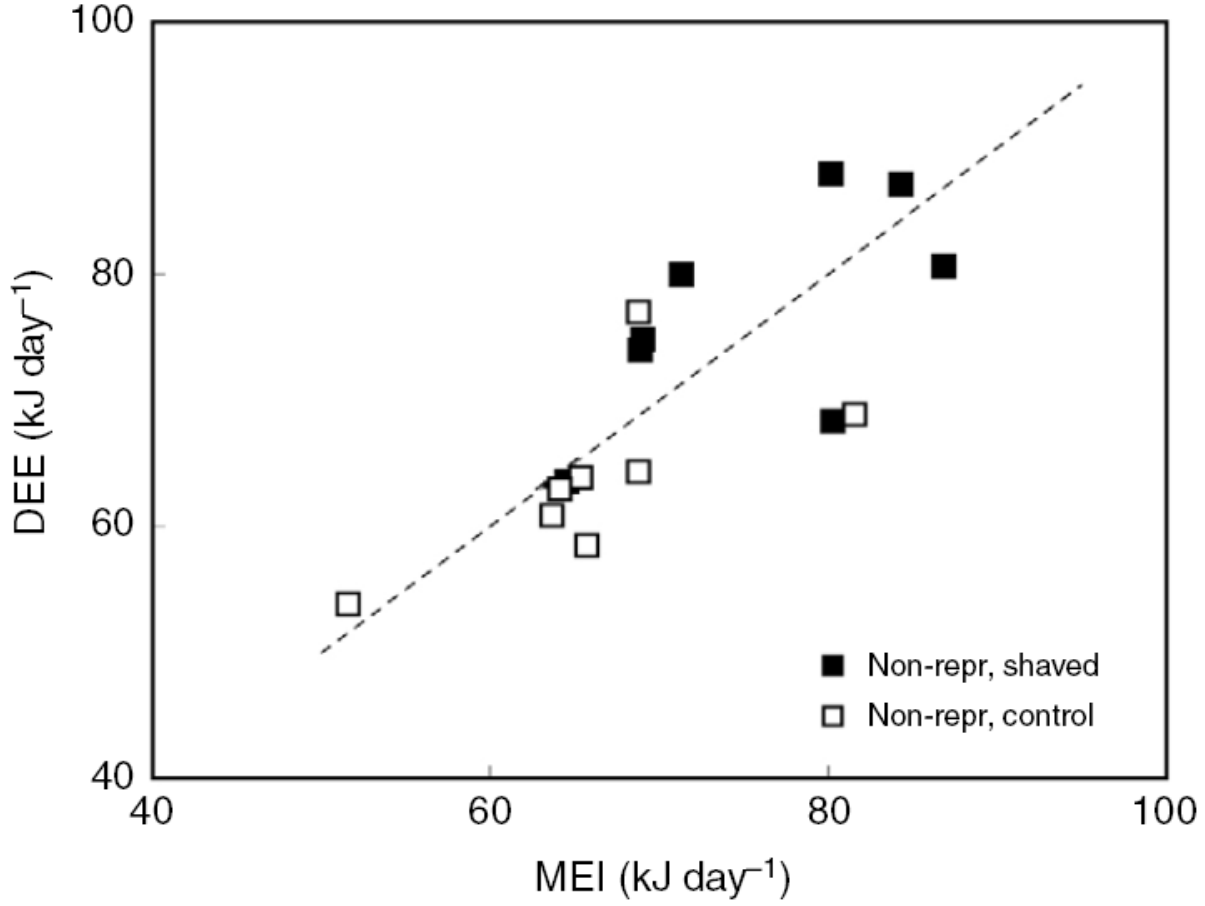

Fig. 3. Relationship between daily energy expenditure (DEE) and metabolizable energy intake (MEI) in non-reproductive shaved (filled squares; *N*=8) and unshaved control (open squares; *N*=8) mice. The line of equality is shown.

Krol et al. 2007. J. exp. Biol. 210, 4233-4243.

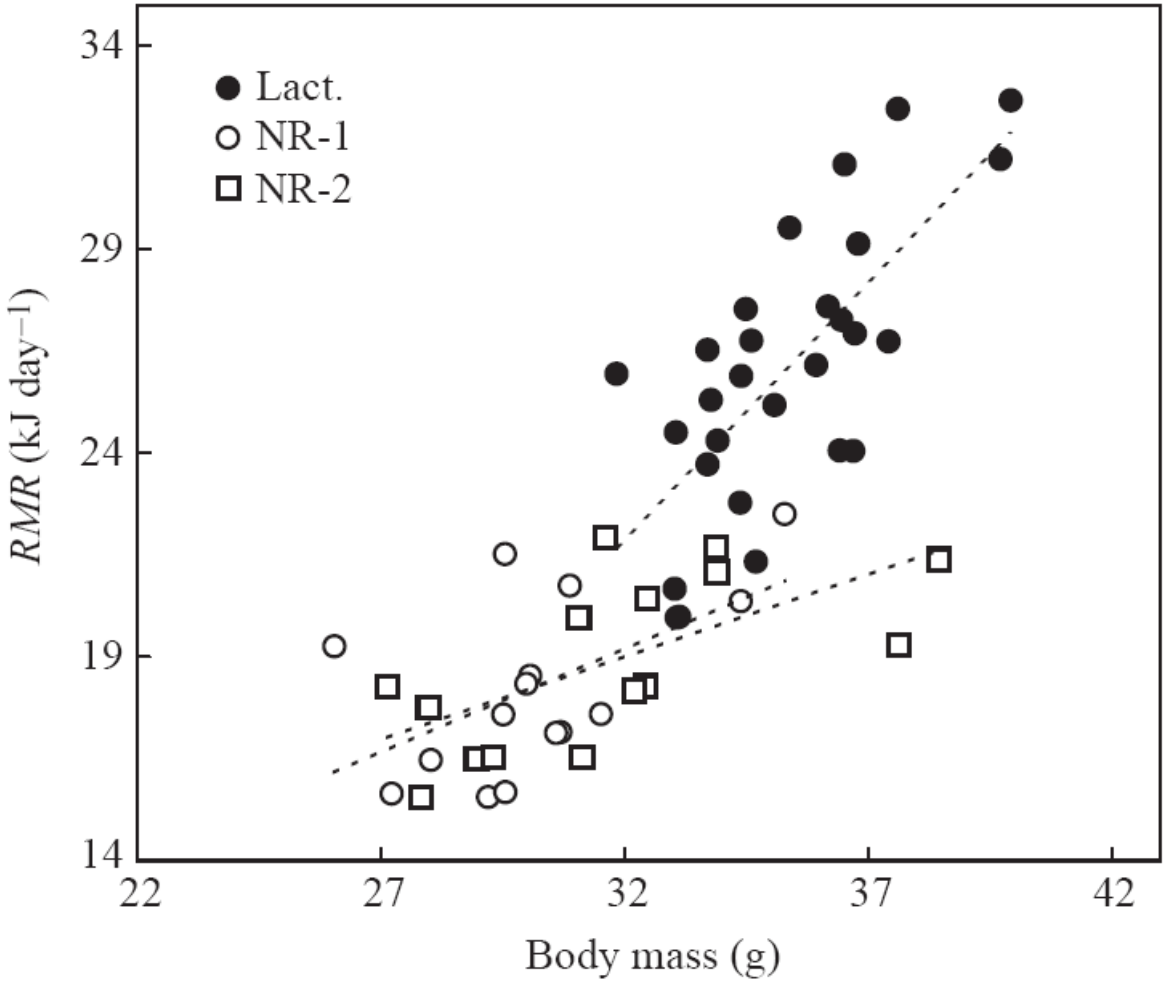

Fig. 1. Resting metabolic rate (*RMR*) as a function of body mass for lactating female mice (filled circles; $y=-18.16+1.25x$; $N=28$) and non-reproductive female mice ($N=15$) measured on two separate occasions: NR-1 (open circles; $y=2.88+0.51x$) and NR-2 (open squares; $y=5.99+0.41x$). Both lactating and non-reproductive mice were exposed to 30°C.

Krol et al 2003. J. exp. Biol. 206, 4283-4291.

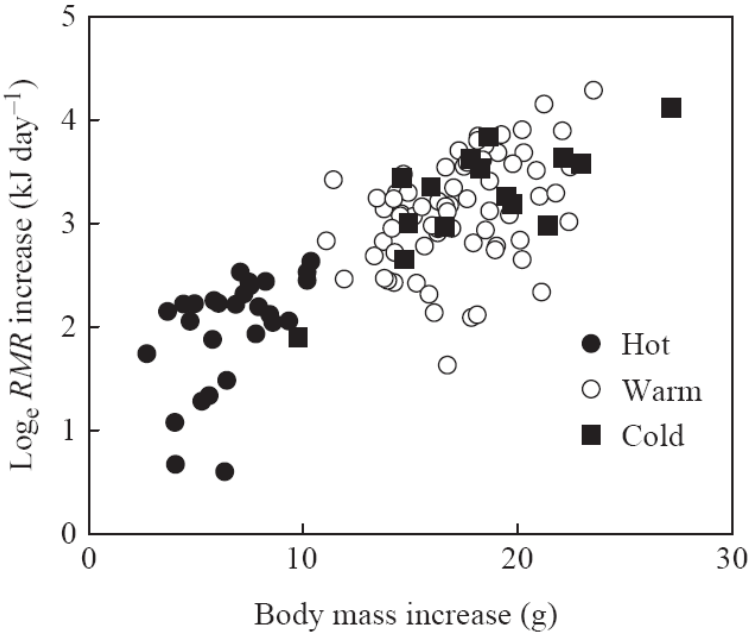

Fig. 3. Relationship between increase in resting metabolic rate (*RMR*) and increase in body mass at peak lactation above the levels measured prior to breeding, in mice exposed to hot (30°C), warm (21°C) and cold (8°C) temperatures (*N* as in text). The differences between the groups are not significant (for statistical details, see Results).

Table 4. *Comparison of dry organ masses of lactating mice exposed to hot (30°C, N=9), warm (21°C, N=16) and cold (8°C, N=15) temperatures*

	Dry organ mass (g)			ANOVA	
Organ	Hot	Warm	Cold	$F_{2,37}$	P
Brown adipose tissue	0.060[a]	0.055[a]	0.136[b]	18.8	**<0.001**
Heart	0.044[a]	0.061[b]	0.078[c]	27.1	**<0.001**
Lungs	0.098[a]	0.081[a]	0.189[b]	13.8	**<0.001**
Stomach	0.085[a]	0.076[a]	0.328[b]	18.7	**<0.001**
Small intestine	0.282[a]	0.314[a]	0.398[b]	9.3	**0.001**
Large intestine	0.120[a]	0.158[a]	0.235[b]	28.9	**<0.001**
Liver	0.599[a]	0.859[b]	1.028[c]	31.3	**0.001**
Pancreas	0.113[a]	0.188[a]	0.292[b]	12.7	**<0.001**
Spleen	0.026[a]	0.022[a]	0.040[b]	18.4	**<0.001**
Kidneys (wet mass, g)	0.433[a]	0.557[b]	0.667[c]	40.3	**<0.001**
White adipose tissue	0.034[a]	0.050[a]	0.516[b]	10.5	**<0.001**
Mammary glands	0.956[a]	1.115[a]	2.450[b]	22.3	**<0.001**
Uterus	0.035	0.056	0.124	5.1	0.011
Tail	0.358[a]	0.324[a]	0.422[b]	28.5	**<0.001**
Pelage	1.467[a]	1.294[a]	1.847[b]	9.1	**0.001**
Carcass	4.331[a]	4.434[a]	5.463[b]	21.6	**<0.001**

Krol et al 2003. J. exp. Biol. 206, 4283-4291.

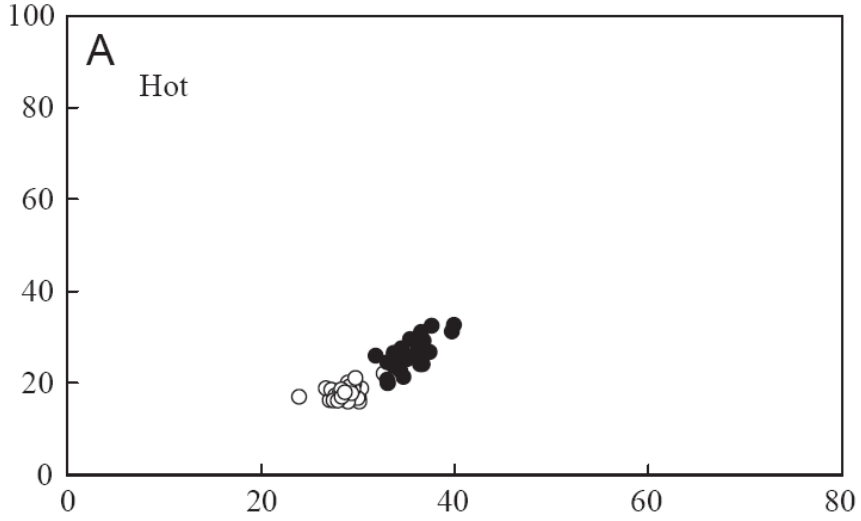

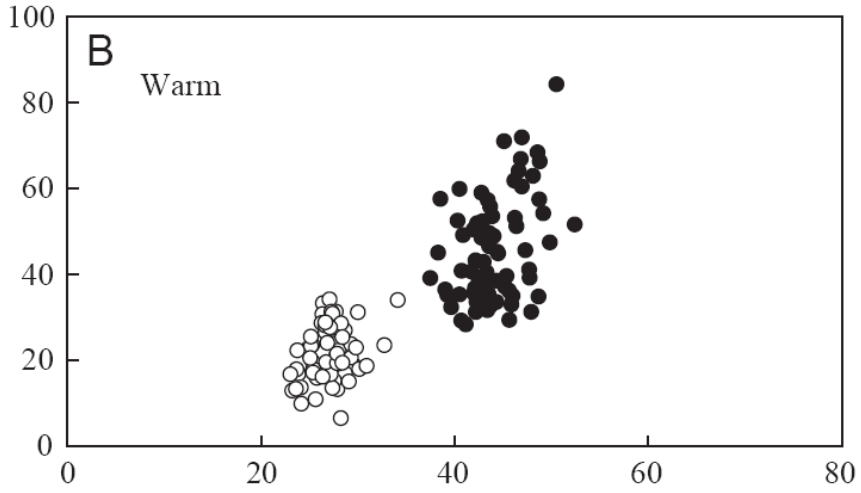

RMR (kJ day^{-1})

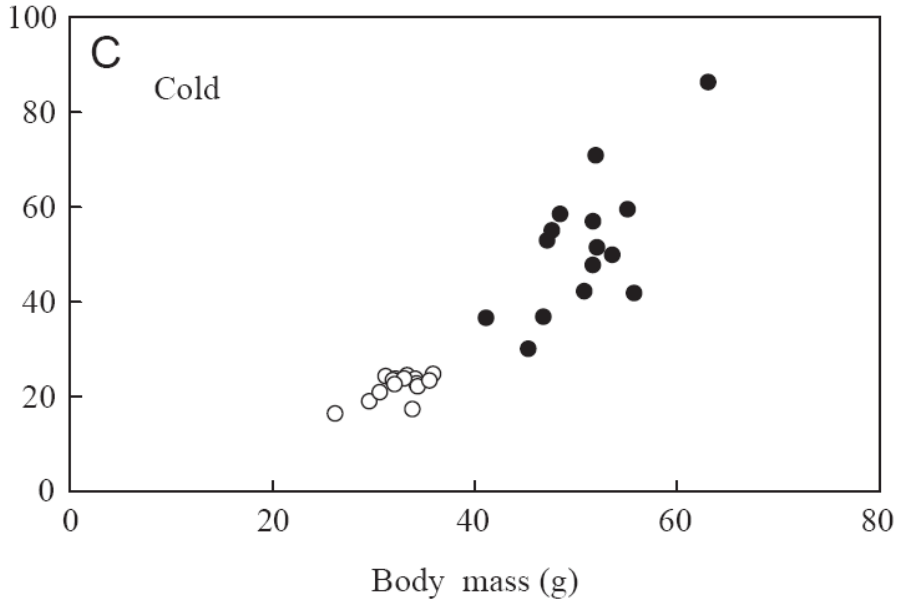

Table 2. *Resting metabolic rate and food intake of mice exposed to hot (30°C,* N=*28), warm (21°C,* N=*71) and cold (8°C,* N=*15) temperatures*

	Mice		
Trait	Hot[a]	Warm[a]	Cold[b]
BM_{PB} (g)[c]	28.6±1.6	27.1±2.1	32.5±2.5
RMR_{PB} (kJ day^{-1})[d]	17.9±1.6	21.5±6.1	22.2±2.6
BM_{L} (g)[c]	35.3±2.0	44.3±3.2	50.8±5.2
RMR_{L} (kJ day^{-1})[d]	26.0±3.5	47.0±13.8	51.8±14.3
BM increase (g)[e]	6.7±2.1	17.1±2.8	18.3±4.2
RMR increase (kJ day^{-1})[f]	8.1±3.3	25.5±13.1	29.6±13.6
Food intake (kJ day^{-1})[g]	194.5±32.0	369.5±40.5	487.8±102.1

Krol et al 2003. J. exp. Biol. 206, 4283-4291.

Mouse litter size

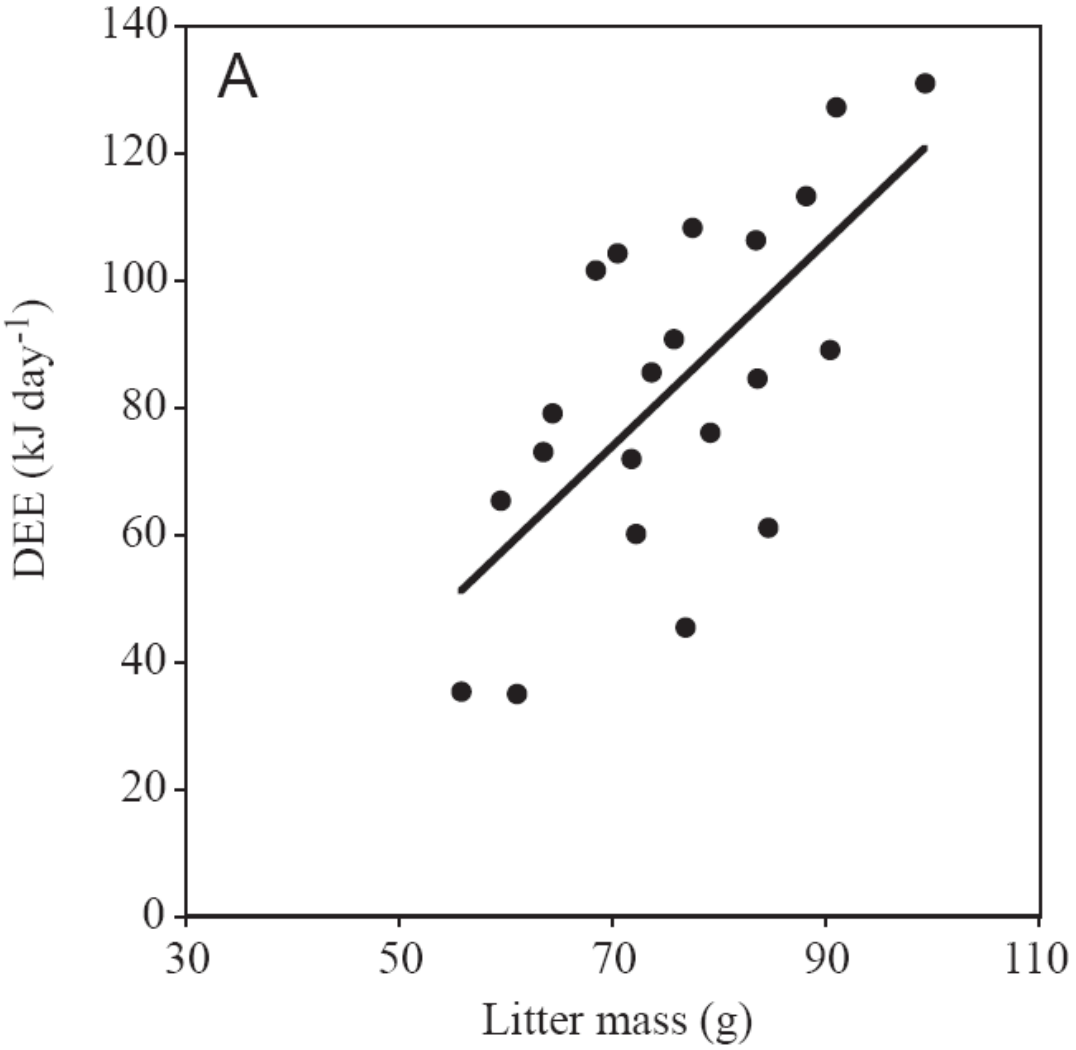

Johnson et al. 2001. J. exp. Biol. 204, 1925-1935.

Fig. 1. Lactating MF1 mouse with dorsal fur shaved off to increase heat loss capacity.

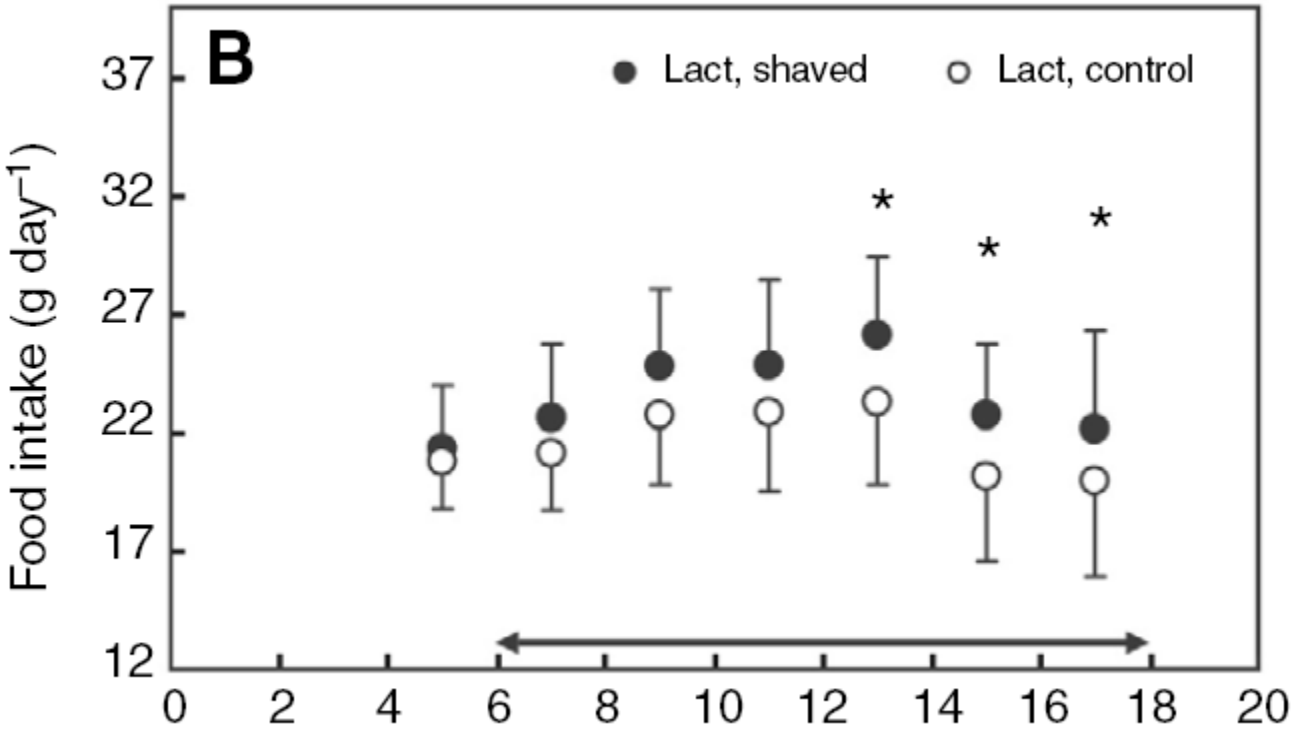
B
Lact, shaved
Lact, control
Food intake (g day⁻¹)
37
32
27
22
17
12
0
2
4
6
8
10
12
14
16
18
20
*
*
*

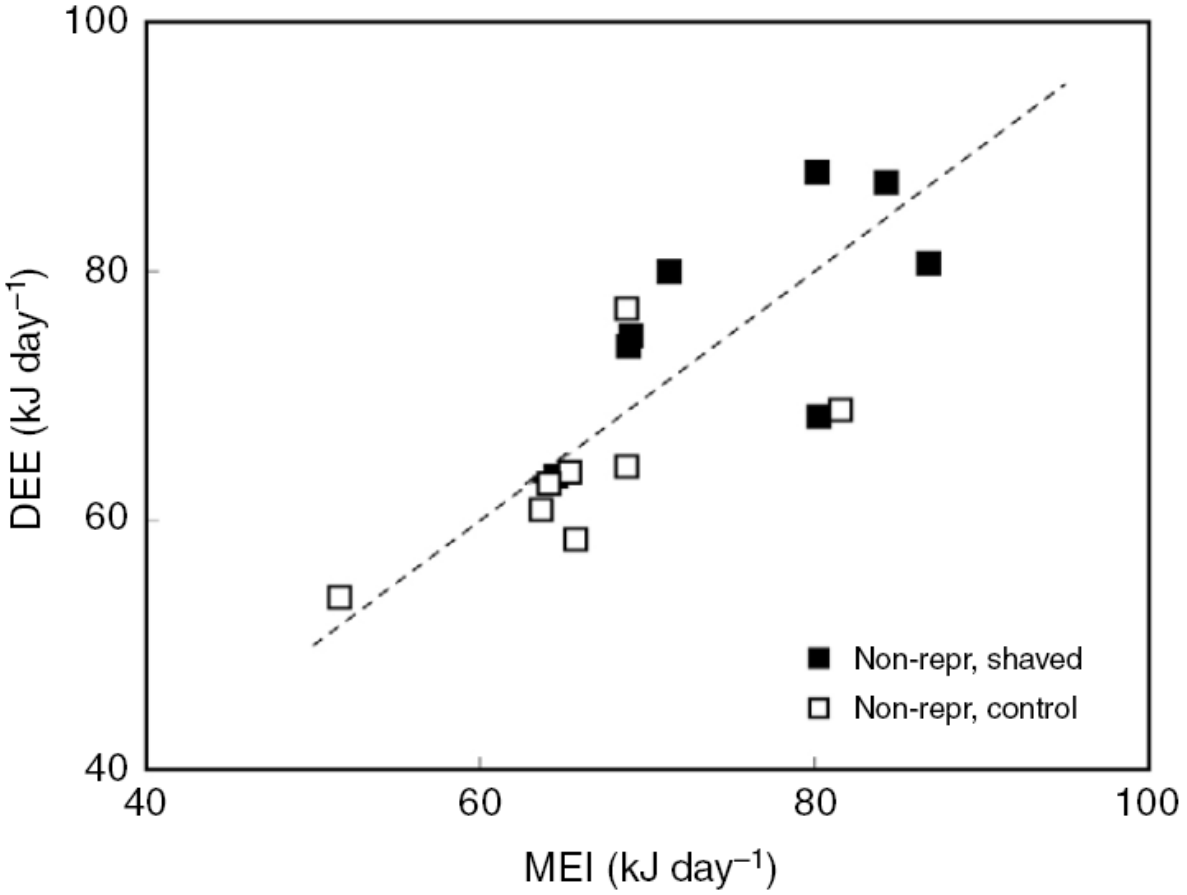

Fig. 3. Relationship between daily energy expenditure (DEE) and metabolizable energy intake (MEI) in non-reproductive shaved (filled squares; N=8) and unshaved control (open squares; N=8) mice. The line of equality is shown.

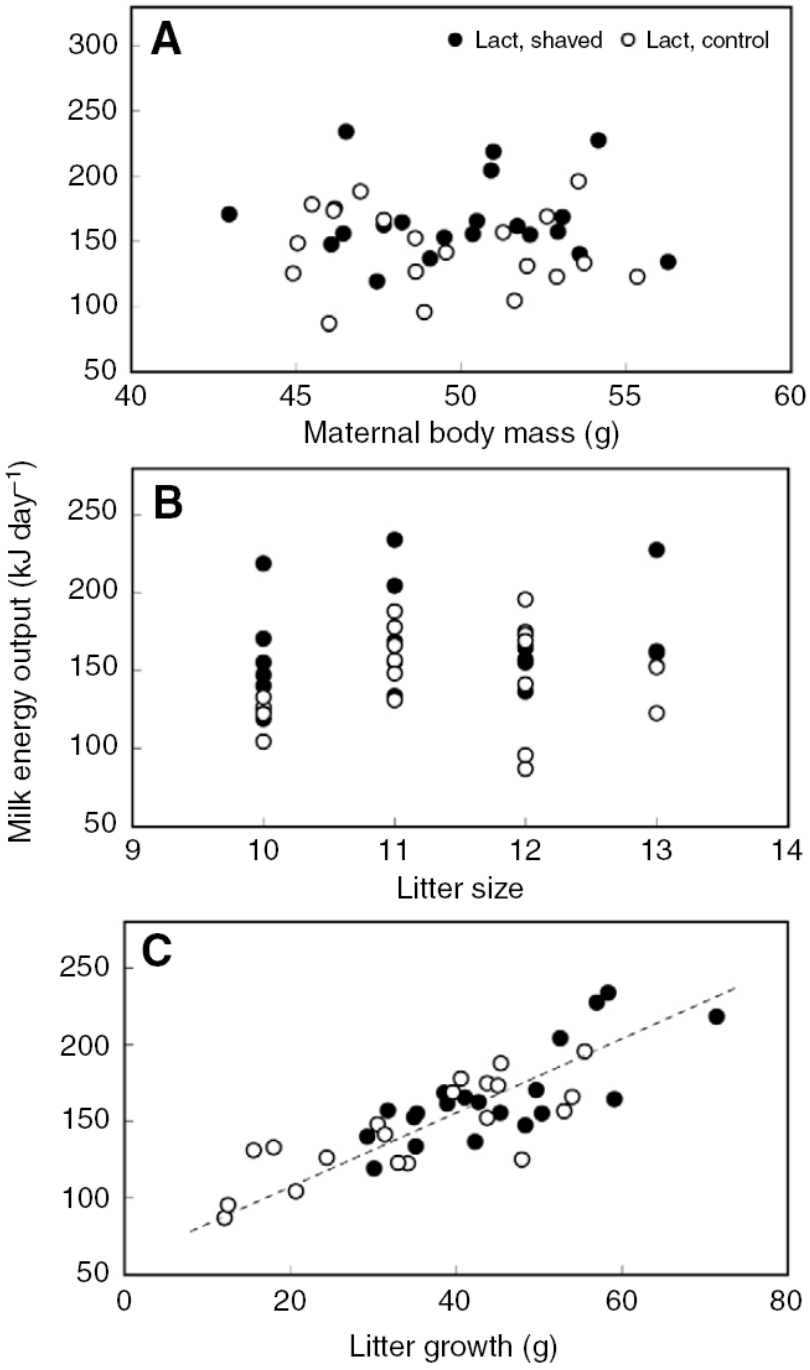
A
Lact, shaved
Lact, control
300
250
200
150
100
50
40
45
50
55
60
Maternal body mass (g)
B
Milk energy output (kJ day⁻¹)
250
200
150
100
50
9
10
11
12
13
14
Litter size
C
250
200
150
100
50
0
20
40
60
80
Litter growth (g)

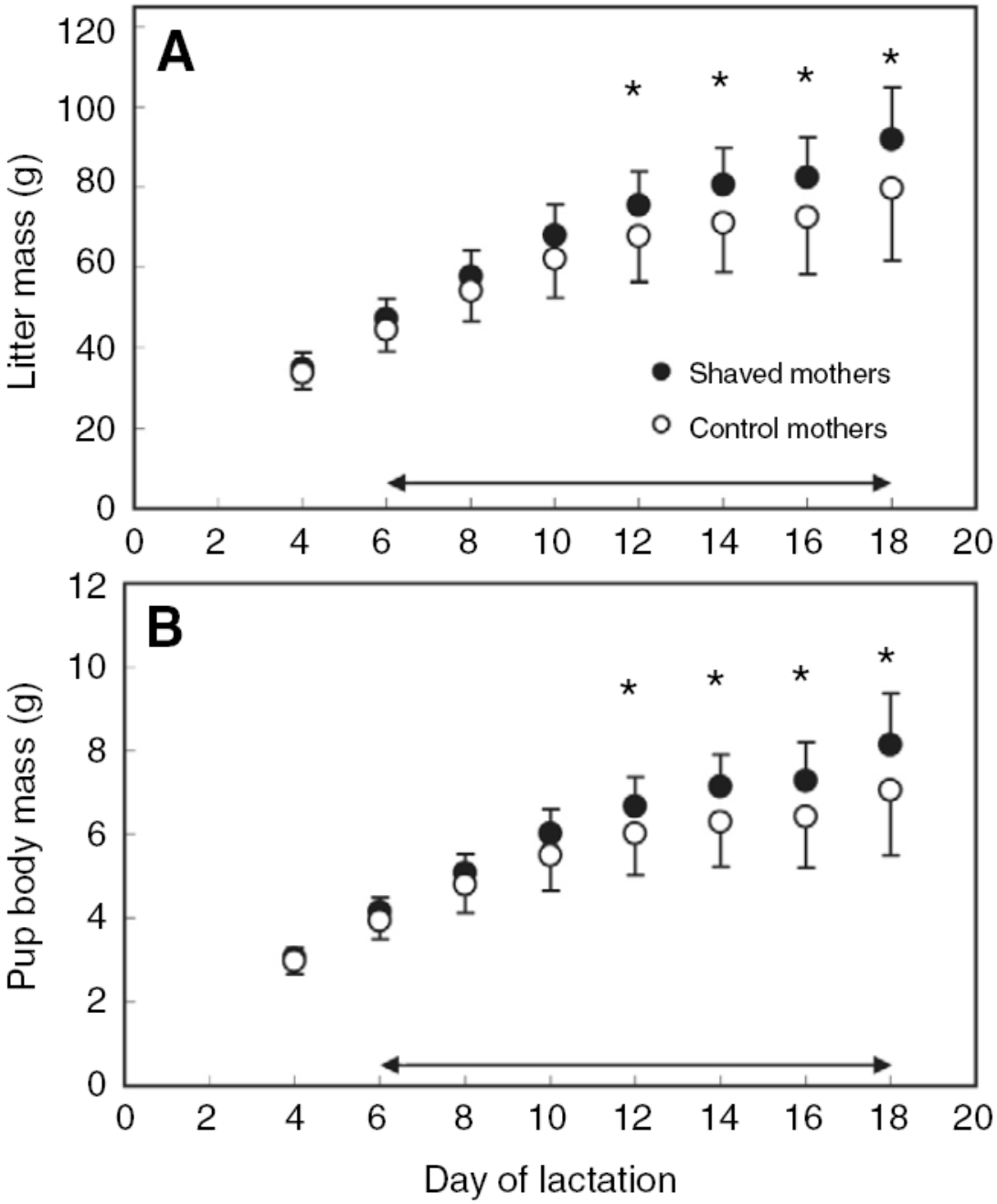
A
B
Litter mass (g)
Pup body mass (g)
Day of lactation
Shaved mothers
Control mothers
0
20
40
60
80
100
120
0
2
4
6
8
10
12
14
16
18
20
*